Optimization of a Hybrid Combination of a Photovoltaic System and a Wind Energy Conversion System:
Izmir Institute of Technology Campus Area Case

By

Orhan EKREN

A Dissertation Submitted to the
Graduate School in Partial Fulfillment of the
Requirements for the Degree of

MASTER OF SCIENCE

Department : Energy Engineering
Major : Mechanical Engineering

Izmir Institute of Technology
Izmir, Turkey

June, 2003

We approve the thesis of **Orhan EKREN**

Date of Signature

09.06.2003

....

Assoc. Prof. Dr. Baris ÖZERDEM

Supervisor

Department of Mechanical Engineering

09.06.2003

....

Assoc. Prof. Dr. Aydogan ÖZDAMAR

Department of Mechanical Engineering

09.06.2003

....

Asst. Prof. Dr. Gülden GÖKCEN

Department of Mechanical Engineering

09.06.2003

....

Prof. Dr. Ing. Gürbüz ATAGÜNDÜZ

Head of Interdisciplinary Energy Engineering

Head of Energy Engineering

ACKNOWLEDGEMENTS

First of all, I particularly would like to thank my advisor, Assoc. Prof. Dr. Baris OZERDEM, for his continuous guidance, support and vision that he never hesitated to share, without which this study would not become a reality.

I also owe a great deal of thanks to Asst. Prof. Dr. Koray ÜLGEN, who I have worked together with throughout the period of this exciting and wonderful study, for sharing his experience with me and for his never ending technical and personal support.

I also would like to take this opportunity to thank   Banu YETKIN EKREN for her support in optimization procedure and personal support.

I sincerely thank my parents, for their support and encouragement.

ABSTRACT

Renewable energy resources have gained the great importance due to the growing concerns of environmental problems. The integrated utilization of renewable energies such as solar and wind are becoming very attractive, especially, in most of the isolated and remote areas in many parts of the world.

In the present study, firstly, wind and solar radiation measurements, made on Izmir Institute of Technology (IZTECH) Campus area, have been analyzed in order to determine the, both, solar and wind energy potentials of the location. The monthly average wind speeds range from 5.7 m/s to 7.7 m/s, the monthly average of daily values of solar radiation range from 2.1 kWh/m^2 to 5.7 kWh/m^2 at the monitoring station throughout the measurement period of 12 months between 01.01.2002 and 31.12.2002.

Secondly, a procedure is described which determines the hybrid system parameters such as photovoltaic (PV) array area and rotor swept area of wind turbine while satisfying a specific load distribution. The employed method is a graphical construction to figure out the optimum configuration of the generators that satisfies the energy demand mentioned above.

ÖZ

Çevre kirliliğinin artmasıyla, yenilenebilir enerji kaynaklarının kullanımı büyük önem kazanmıştır. Dünyanın birçok yerinde özellikle şebekeden uzak yerlerde güneş ve rüzgar gibi yenilenebilir enerji kaynaklarının birlikte kullanımı önemli hale gelmiştir.

Bu çalışmada; ilk olarak, İzmir Yüksek Teknoloji Enstitüsü Kampüs alanında rüzgar ve güneş enerjilerinin potansiyelini belirleyebilmek amacıyla, rüzgar hızları ve güneş radyasyonu ölçümleri yapılmış ve elde edilen veriler analiz edilmiştir. 01.01.2002 ve 31.12.2002 tarihleri arasındaki 12 aylık sürede yapılan ölçümler sonucunda, aylık ortalama rüzgar hızlarının 5.7 m/s ile 7.7 m/s aralığında, aylık ortalama güneş radyasyonunun ise 2.1 kWh/m^2 ile 5.7 kWh/m^2 arasında değiştiği gözlenmiştir.

Daha sonra, belirlenen bir ihtiyacı karşılayacak hibrid sistem parametreleri olan fotovoltaik yüzey alanı ve rüzgar türbini rotor süpürme alanı hesaplanmıştır. Belirlenen ihtiyacı tam olarak karşılayacak optimum üreteç konfigürasyonu da grafik yöntem kullanılarak elde edilmiştir.

TABLE OF CONTENTS

LIST OF FIGURES

LIST OF TABLES

NOMENCLATURE

Chapter 2

b	Refer to beam radiation
d	Refer to diffuse radiation
G_{sc}	Solar constant (W/m^2)
G_{on}	Extraterrestrial radiation on a plane normal to direction (W/m^2)
G_o	Extraterrestrial radiation on horizontal plane (W/m^2)
H	Insolation for a day (Wh/m^2)
H_o	Daily extraterrestrial insolation on a horizontal surface (Wh/m^2)
$\underline{H}_o$	Monthly average of daily total extraterrestrial solar insolation on horizontal surface (Wh/m^2)
I	Insolation for an hour (Wh/m^2)
N	The number of days from January 1
N_m	The day of year
n	Refer to radiation on a plane normal to direction
o	Refers to extraterrestrial radiation above the earth's atmosphere
T	Refer to radiation on tilted plane
WRC	World Radiation Center
α_s	Solar altitude angle (in degree)
β	Surface altitude angle (in degree)
γ	Surface azimuth angle (in degree)
γ_s	Solar azimuth angle (in degree)
δ	Solar declination (in degree)
θ	The solar incident angle (in degree)
θ_z	The zenith angle (in degree)
ϕ	Latitude (in degree)
ω	Hour Angle (in degree)
$\omega_{sunrise}$	Sunrise times
ω_{sunset}	Sunset times
_	Means monthly average of daily total

Chapter 3

a	Interference factor
A_1	Cross-sectional area of stream (m^2)
F	Axial force on the turbine
P_{tot}	Total wind power (W)
P_0	The power in the unperturbed wind (W)
P_T	Power extracted by turbine (W)
P_W	Power extracted from wind (W)
$\dot{m}$	Mass-flow rate (kg/s)
z_0	The roughness length (m)
α	Exponential wind gradiant
C_p	Theoretical wind generator efficiency (%)
ρ	Air density (kg/m^3)
V_0	Upstream wind speed (m/s)
V_1	Wind speed at rotor (m/s)
V_2	Downstream wind speed (m/s)

Chapter 4

AC	Alternative current
DC	Direct current
mV	Milivolt
PV	Photovoltaic
GND	Ground

Chapter 5

DMI	Turkish State Meteorological Sevice
EIEI	General Directorate of Electrical Power Resources Survey and Development Administration
ESRA	European Solar Radiation Atlas

$\underline{H}$	Monthly average of daily total radiation on horizontal surface (Wh/m^2)
$\underline{H}_T$	Monthly average of daily total radiation on tilted surface (Wh/m^2)
$\underline{H}_d$	Monthly average of daily total diffuse radiation on horizontal surface (Wh/m^2)
H_d	Total diffuse radiation
H_b	Total beam radiation
$\underline{K}_T$	Monthly average clearness index
$^L{}_O$	Low
R	Total radiation tilted factor
R_B	Beam radiation tilt factor
WMO	World Meteorological Organisation
ω_{sunset}'	Sunset hour angle on tilted surface (in degree)
r	Average reflectivity

Chapter 6

Day	Total day of month
D	Duration of 1 day (24 hours.)
h	Height from sea level (m)
W	Monthly average of daily total wind energy (Wh/m^2)
V_i	Incoming velocity (m/s)
A	Cross-sectional area of stream (m^2)

Chapter 7

A_s	Photovoltaic cell area (m^2)
A_w	Wind turbine swept area (m^2)

c_j	Increase in z that would result from each unit increase in level of activity j $(j= 1,2,...,n)$
b_i	Amount of resource i that is available for allocation to activities $(i=1,2,..,m)$
a_{ij}	Amount of resource i consumed by each unit of activity j $(j=1,2,...,n)$
a_s	Coefficient in Equation (7.9)
a_w	Coefficient in Equation (7.10)
C_h	Total cost per unit power potential of hybrid generator
C_s	Cost per unit power potential of solar generator
C_w	Cost per unit power potential of wind generator
d	Power demand (W/m^2)
g	Subject function
LP	Linear Programming
LINDO	Linear Interactive Discrete Optimizer software
r	Radius of rotor (m)
W_p	Peak- watt
z	Value of overall measure of performance
x_j	Level of activity j $(j= 1,2,...,n)$
η	Module efficiency (%)

CHAPTER 1
INTRODUCTION

The importance of renewable energy supplies are increasing steadily in all over the world. Renewable energy is energy obtained from the continuing or repetitive currents of energy occurring in the natural environment. Non–renewable energy, on the contrary, is energy obtained from static and isolated stores of energy that remain bound unless released by human interaction. Non-renewable energy is called fossil fuel energy also [1].

There are three ultimate sources of energy:

1. the sun.
2. the motion and gravitational potential of the planet.
3. the earth.

Renewable energy is derived from any of those sources. Source of the all renewables such as solar, hydrolic, ocean thermal, wind, wave and bio energies, except tide and geothermal energies, is the sun. Renewable energy resources have limited negative impacts to the environment when comparing with fossil fuel resources. Besides their limited resources fossil fuels have negative environmental impacts such as air pollution, acid rain and ozon depletion. Renewable energy is abundant, well established technology and a domestic resource which has potential to contribute or provide complete security of supply [2,3].

Total energy use per capita is 0.8 kW in the world. This value is 10 kW in USA, 4 kW in Europe and 0.1 kW in Africa. Since the world population doubles in every 20-30 years the growth of world supply should be between 4-8 % per year [1]. Without new and renewable energy supplies such growth can not be maintained. It must be noted that suppling the total demand of energy from renewable resources for any country is impossible. When we look at the situation of Turkey in terms of energy resources, it does not possess enough conventional fossil fuel reserves. Contrary to this fact, it possesses rich renewable energy resources such as hydrolic, solar, geothermal and wind.

Turkey is geographically well situated with respect to solar energy potential that is about 2640 hours per year. Average daily solar energy density is 3.6 kWh/m^2. The total gross solar energy potential of Turkey is calculated to be about 88 mtoe (million tons of oil equivalent), of which 40% can be used economically.

Three-fourths of the economically usable potential is efficient for thermal use and the remainder for electricity production [4]. In 1999 and 2000, solar energy use accounted for 112 ktoe (kilo tons of oil equivalent) and 129 ktoe, respectively. It is expected to reach 431 ktoe in 2010 and 828 ktoe in 2020 [5,6]. The yearly average total solar radiation varies from a low of 1120 kWh/(m^2.yr) in the Black Sea Region with 1971 hours of sunshine a year to a high of 1460 kWh/(m^2.yr) in the South East Anatolian with 2993 hours of sunshine a year. Although Turkey has high solar potential, residential and industrial utilization of solar energy started in the 1980s. The residential sector accounted for the biggest share at about three times larger the consumption of the industrial sector between 1986 and 1998 in Turkey.

A reasonably accurate knowledge of the availability of the solar resource at any place is required by solar engineers, architects, agriculturists and hydrologists in many applications of solar energy such as solar furnaces, concentrating collectors, and interior illumination of buildings [7,8,9,10]. On the other hand, the determination of solar energy capacity effectively through the empirical models plays a key role in developing solar energy technologies and the sustainability of natural resources [11]. For this purpose, in the past, several empirical formulas using various parameters have been tested in order to estimate the solar radiation around the world [12,13,14,15,16,17,18]. These parameters include extraterrestrial radiation, sunshine hours, relative humidity, ambient temperature, and soil temperature, number of rainy days, altitude, latitude and cloudiness. Based on the studies carried out in Turkey, some researchers gave the correlations for some provinces of Turkey such as Elazig, [8]; Trabzon, [9]; Gebze [10]; Antalya, [11]; Izmir, [19]; and also for Turkey's general values. Photovoltaic system consist of solar cells. Solar cells are made from semiconductors and have much in common with other solid-state electronic devices, such as diodes, transistors and integrated circuits. For practical operation, solar cells are usually assembled into modules [7,8,20,21].

Among the renewable alternatives, wind energy plays a crucial role and wind farms are becoming widely used all over the world. Wind energy was used more than 5000 years ago, whether in boats to transport goods in Egypt or to grind seeds to produce flour. It is a clean source of energy, abundant in most parts of the world, low in cost, sustainable, safe, and popular and can create jobs. Wind resources in the developing countries are sufficient to produce thousands of MW power in Asia and Latin America.

Ample attention is directed toward the use of wind energy, especially, after the major energy crisis in 1973 [2,22]. Wind power continues to be the fastest growing power generating technology in the world. Although only about 31128 MW of capacity has presently been installed worldwide by the year 2002 [23,24]. Energy harnessed from the wind has been growing by yearly average of 31 % between 1995-2002. But fraction of wind power in global consumption of electricity is still small [25]. Table1.1 shows the growth of wind power in a world wide generation context.

Table 1.1 Growth of Wind Power in a World Wide Generation Context [25,26,27].

Year	Wind Power		All Electricity Generation Capacity	
	Capacity GW	**Energy** TWh	**Capacity** GW	**Energy** TWh
1996	607	1223	(3159)	(13613)
1997	764	1539	3221	13949
1998	1015	2125	3298	14340
1999	1393	2818	3377	14741
2000	1843	3730	3458	15153
2001	2493	5027	3540	15577
2011(est.)	1794	40867	4386	19989

In this regard, electricity production through wind energy for Turkey was realized for the first time at Cesme Altinyunus Resort Hotel, Izmir in 1986 by using a 55 kW nominal powered wind turbine. The First Build-Operate-Transfer (BOT) wind farm, located at Alacati, Izmir, was commissioned in November 1998. This wind power plant has 12 wind turbines with a total installed capacity of 7.2 MW. Second wind farm established in the form of autoproducer was erected in Germiyan, Izmir with a total installed capacity of 1.74 MW. The third wind farm was built in Bozcaada, Canakkale with a total installed capacity of 10.2 MW so, up to date, total installed capacity of 19.13 MW with those three wind farms [28]. It is very important for the wind industry to be able to describe the variation of wind speeds. Wind energy conversion system designers need the information to optimize the design of their systems, so as to minimize generating costs. Over the last decade, various researchers have carried out a number of studies in order to assess wind power around the world [29,30,31,32,33,34].Based on the studies carried out in Turkey, some researchers have performed the assessments of wind power in western Turkey on the basis of individual locations [35,36,37,38,39].

Photovoltaic energy and wind energy conversion systems have been widely used for electricity supply in isolated locations far from the distribution network. These

systems provide a reliable service, and can operate in an unattended manner for extended periods of time if they may be well designed. However, these systems suffer from the fluctuating characteristics of available solar and wind power sources, and this feature must be considered in the design of the system [40,41]. The cost of the individual system is also closely related to their size. Therefore, optimum size distribution in a hybrid system is an important aspect. Many parameters such as meteorological data, cost of components, and a temporal distribution of the electric load must be taken into account in the design [42].

The main objectives of the present study are;

- to overview the potential of both solar and wind energy capacity and,

- to determine the optimum wind/solar combination of a hybrid system designed by using the meteorological data measured on the Izmir Institute of Technology Campus Area which is located in Urla- Izmir, Turkey.

This thesis is composed of eight chapters. In order; Chapter 2 covers parameters used in calculation of the sun position in the form of astronomical equations meticulously.

Chapter 3 is concerned with the wind energy. Firstly, general rules of the wind energy system. Next, effects of obstacles, hight for the wind speed. Last, equations of the power extracted from the wind.

Chapter 4 consists of implementation details of the wind/solar hybrid energy system. Such components as photovoltaic panel, wind turbine specifications are expressed one by one.

Chapter 5 is concerned with the calculation of solar energy on the tilted surface and solar radiation measuring system. Such components as pyranometer, datalogger specifications are expressed one by one.

Chapter 6 is concerned with the calculation of wind energy at the site and wind speed measuring system. Such components as anemometer, wind vane, thermometer specifications are expressed one by one.

Chapter 7 is concerned with the size optimization procedure of the wind/solar hybrid energy system.

Finally, in Chapter 8, conclusions are presented.

CHAPTER 2

SOLAR RADIATION FROM THE SUN

Due to the spin of the earth about its own axis and its orbiting around the sun, position of the sun varies throughout the day and the season. The Sun rises south of due east in winter and north of due east in summer, and the sun's path is higher in the sky in summer than it is in winter [43].The amount of electricity a PV cell produces depends on its size, its conversion efficiency, and the intensity of the light source which is radiation from the sun [22]. So we should know radiation comes from the sun to the earth surface.

2.1. Components of Solar Radiation

As the name implies, solar radiation is the radiation created by the sun. When the solar radiation passes through the earth's atmosphere, it is partially absorbed. Total or global solar radiation received at ground level consists of direct and indirect radiation, shown in Figure 2.1.

- Beam or direct radiation
- Diffuse or scattered radiation
- Albedo or reflected radiation
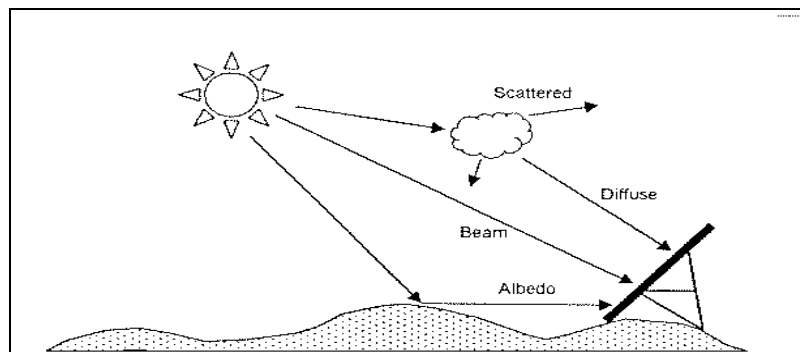
Figure 2.1 Solar Radiation Types at Ground Level [44].

Sunlight reaching the earth surface, which is not reflected or scattered and reaches the surface directly in line, is termed beam or direct radiation. It is the type of sunlight that casts a sharp shadow, and on a sunny day it can be as much as 80 % of the total sunlight striking a surface [41,45,46,]. Hence, beam or direct radiation is the most important type of radiation for solar processes.

Diffuse radiation is the second type of solar radiation. The solar radiation received from the sun after its direction has been changed by scattering by the atmosphere. Diffuse radiation is referred to in some meteorological literature as sky radiation or solar sky radiation [47]. This is such sunlight that comes from all directions in the sky dome other than the direction of the sun. It is the sunlight scattered by atmospheric components such as particles, water vapor, and aerosols. On a cloudy day, the sunlight is 100 % diffuse [48].

Reflected radiation is the third type of radiation. Incoming solar radiation striking the earth surface is partially reflected and partially absorbed. Earth surface reflectivity varies with covering material type. For solar collectors mounted on the roof of a building, the amount of reflected radiation may relatively be small compared to other radiation types [48].

The solar constant, G_{sc} ,is the energy from the sun , per unit time ,received on a unit area of surface perpendicular to the direction of propagation of the radiation, at mean earth-sun distance, outside of the atmosphere [43,47]. The World Radiation Center (WRC) has adopted a value of solar constant 1353 W/m^2 [49].

2.2. Extraterrestrial Radiation

Solar radiation reaching the earth atmospher, which is unmodified by the atmosphere, or radiation outside of the Earth's atmosphere is named extraterrestrial solar radiation [41]. A standart spectral irradiance curve has been compiled based on high altitude and space measurements. The World Radiation Center (WRC) standart is shown in Figure 2.2
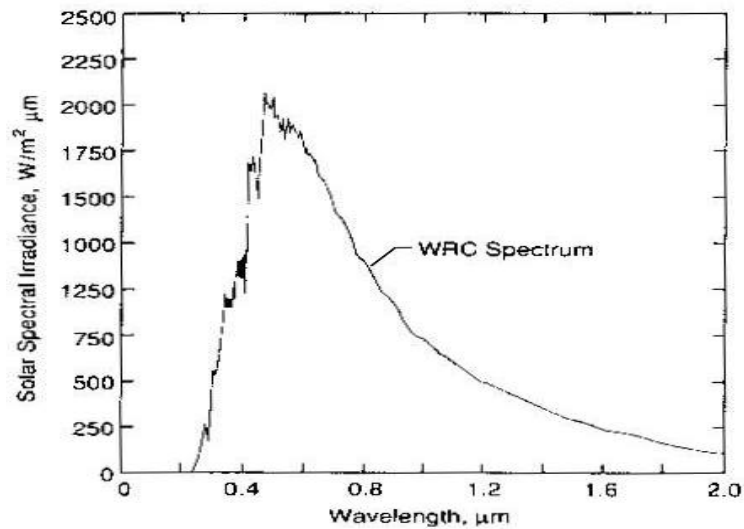
Figure 2.2 Spectral Irradiance Curve at Mean Earth-Sun Distance [47].

Variation of the earth-sun distance, however, does lead to variation of extraterrestrial radiation flux in the range of ± 3 % [43,47]. The dependence of extraterrestrial radiation through out the year is indicated by this equation and is shown in Figure 2.3.

$$G_{on} = G_{sc} \ [\ 1 + \ 0.033 * Cos \ \left(\frac{360\,N}{365} \right)]$$ (2.1)
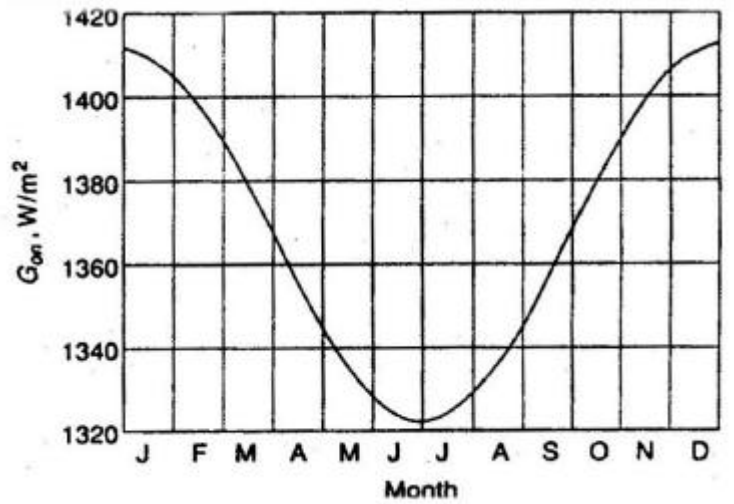
Figure 2.3 Variation of Extraterrestrial Solar Radiation with Time of Year [47].

G_{on} is the extraterrestrial radiation, measured on the plane normal to the radiation on the   N th day of the year.

Irradiance is the measure of the power density of sunlight and is measured in W/m^2 . Irradiation is the measure of energy density of sunlight and is measured in kWh/m^2 . Insolation is a term applying specifically to solar energy irradiation. The symbol H is used for insolation for a day. The symbol I is used for insolation for an hour or other period if specified .

The symbols H   and   I   can   represent beam, diffuse, or total and can be o surfaces of any orientation. Subscripts on G, H, I are as follows: **o** refers to radiation above the earth's atmosphere, referred to as extraterrestrial radiation; **b** and **d** refer to beam and diffuse radiation.

 T and **n** refer to radiation on tilted plane and on a plane normal to direction of propagation. If neither **T** nor **n** appear ,the radiation is on a horizontal plane [47].

2.2.1. Extraterrestrial Radiation on a Horizontal Surface

If there were no atmosphere theoretically possible radiation on a horizontal surface. At any point in time, the solar radiation incident on a horizontal plane outside of the atmosphere is the normal incident solar radiation as given by equation;

$$G_o = G_{sc}\ [\ 1 +\ 0.033 * Cos\ \left(\frac{360\,N}{365}\right)]\ Cos\ \theta_z \tag{2.2}$$

$$G_o = G_{sc} \; [\; 1 + \; 0.033 * \text{Cos} \; \left(\frac{360 \, N}{365} \right)] \; (\text{Cos} \; \phi \; \text{Cos} \; \delta \; \text{Cos} \; \omega + \text{Sin} \; \phi \; \text{sin}\delta \;) \qquad (2.3)$$

It is often necessary for calculation of daily solar radiation to have the integrated daily extraterrestrial radiation on a horizontal surface, H_o . This is obtained by integrating Equation 2.4 over the period from sunrise to sunset.

$$H_o = [24 * G_{sc} * \frac{0.0036}{p}] * [1 + 0.033 * \text{Cos} \; \left(\frac{360 \, N_m}{365} \right)] * [\cos \phi \; \cos \delta \; \sin \omega_{sunset} +$$

$$\pi * \frac{w_{sunset}}{180} * \text{Sin}\phi \; \text{Sin} \; \delta] \qquad (2.4)$$

$$\underline{H_0} = (\frac{\sum H_0}{\text{total number of the day for the month}}) \qquad (2.5)$$

$\underline{H}_o$ is monthly average daily total extraterrestrial solar radiation on horizontal surface calculated by using Mathlab software and these data are given in Table 2.1.

Table 2.1 Monthly Average of Daily Total Extraterrestrial Radiation on Horizontal

Surface

Latitude	Month	$\underline{H}_o$ (Wh/m^2)	$\underline{H}_o$ (MJ/m^2)
38°	January	4583.3	16.5
38°	February	5944.4	21.4
38°	March	7861.1	28.3
38°	April	9750	35.1
38°	May	11055.6	39.8
38°	June	11583.3	41.7
38°	July	11305.6	40.7
38°	August	10250	36.9
38°	September	8527.8	30.7
38°	October	6527.8	23.5
38°	November	4888.9	17.6
38°	December	4166.7	15.0
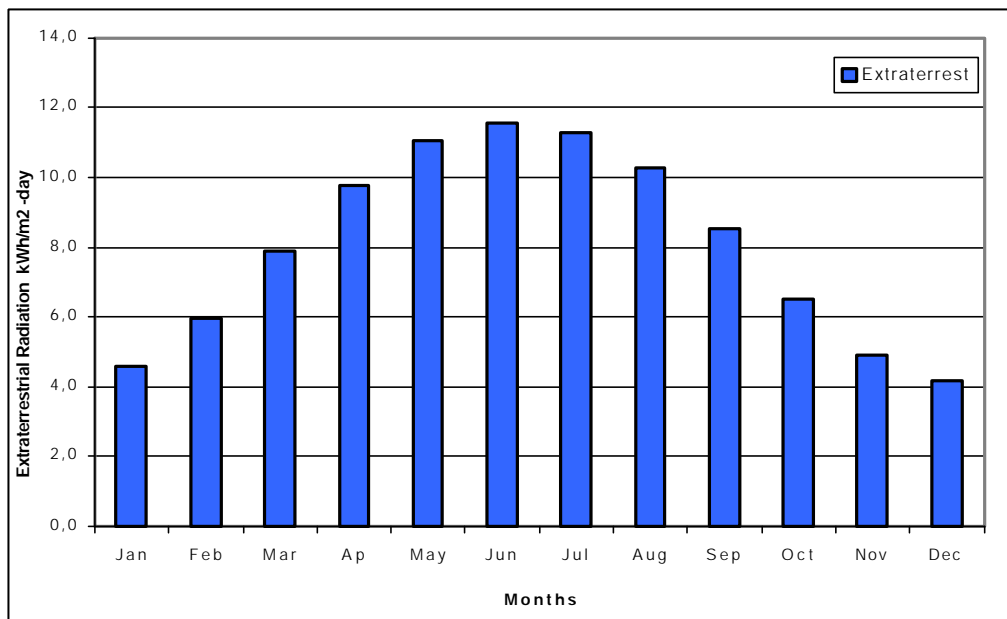
Figure 2.4 Monthly Average of Daily Total Extraterrestrial Radiation on Horizontal
Surface.

2.3. Geometry of the Earth and Sun

2.3.1. Latitude (ϕ) and Longitude

Latitude ϕ is a scale used to measure one's location on the earth, north or south of the equator. Latitude values for points south of the equator are always negative, and values for points north of the equator are always positive as shown in Figure 2.5.
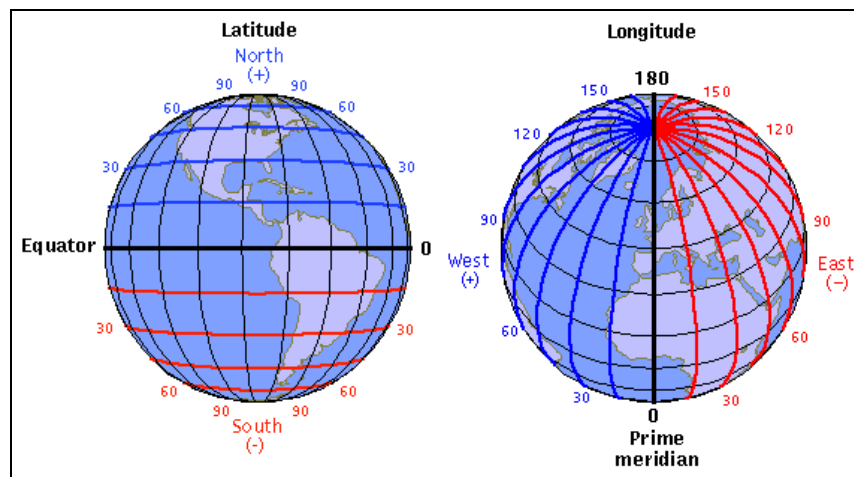
Figure 2.5 Latitude and longitude [50].

The longitude is a scale used to measure one's location on the earth, east or west of the Greenwich Meridian. The Greenwich Meridian is 0° longitude. Longitude values for points east of the Greenwich Meridian are always negative, while points west of the Greenwich Meridian are always positive as shown in Figure 2.5.

2.3.2. Solar Declination (δ)

The solar declination δ, as shown in Figures 2.6 and 2.7, is the angle between the sun-earth center-to-center line and the projection of the same line on the equatorial plane [45].

11
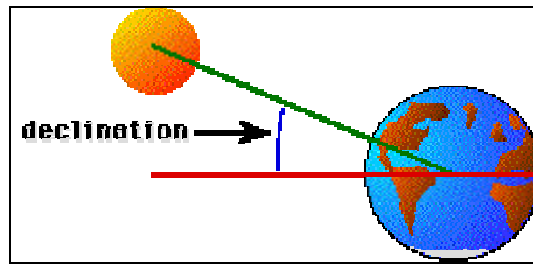
Figure 2.6 The Declination Angle [51].

As shown in Figure 2.6, the value of declination of the sun ranges from 0° at the spring equinox, to $+23.5^o$ at the summer solstice, to 0° at the fall equinox, to -23.5^o at the winter solstice [43].
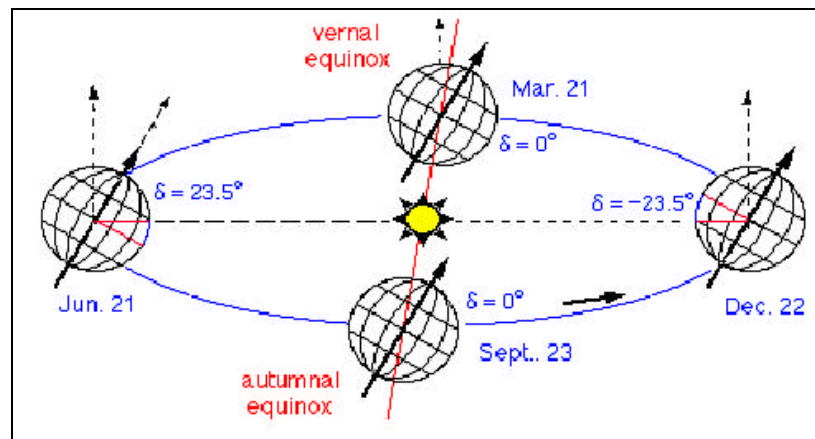
Figure 2.7 Variation Of Declination Angle in a Year[43].

The declination angle, in degrees, for any time of a day can be calculated using by the Equation 2.5

$$\delta = 23.45 * Sin\,[\frac{360*(284+N)}{365}]\qquad\qquad(2.6)$$

where,

δ = Declination
N = Day number, January 1 = day 1.

Average day (N_m) of the month is used while to calculate monthly average of daily total solar radiation.

Table 2.2 Recommended Average Days for Months and Values of N by Months [47].

Month	N for i th Day of Month	For the Average Day of the Month		
		Date	N_m, Day of year	δ, Declination (^{o})
January	i	17	17	-20.9
February	$31+i$	16	47	-13.0
March	$59+$	16	75	-2.4
April	$90+i$	15	105	9.4
May	$120+i$	15	135	18.8
June	$151+i$	11	162	23.1
July	$181+i$	17	198	21.2
August	$212+i$	16	228	13.5
September	$243+i$	15	258	2.2
October	$273+i$	15	288	-9.6
November	$304+i$	14	318	-18.9
December	$334+i$	10	344	-23.0

2.3.3. Slope (β)

The angle between the plane of surface and the horizontal, $0 \leq \beta \leq 180\ ^o$. $\beta \geq 90\ ^o$ means that the surface has a downward facing component.Slope angle is shown in Figure 2.8.

$$\beta = \phi - [1.5 * \delta\,] - \left[\frac{(|d| * f)}{180} \right] \qquad (2.7)$$

Also, the declination must be used which is calculated by using the average day (N_m) of the month while to calculate monthly average of daily total solar radiation.

2.3.4. Hour Angle (ω)

The hour angle is an expression describing the difference between local solar time and solar noon. Although it is calculated directly from measurements of time, it is expressed in angular units in degrees. The hour angle measures time before solar noon in terms of one degree for every four minutes [43].

$$\omega = \pm\ ^{15}\!/_{60} * \text{(Number of minutes from local solar noon)} \qquad (2.8)$$

It must be noted that, the "+" sign applies to afternoon hours and "–" sign to morning hours [43,47].

2.3.5. Sunrise and Sunset

Sunrise and sunset are defined as morning and evening times that the sun is apparent at the horizontal. The sun would normally appear to be exactly on the horizon when its altitude angle is zero degrees, except that the atmosphere refracts sunlight. The observer's elevation relative to surrounding terrain also impacts the apparent time of sunrise and sunset. Sunrise and sunset times are calculated by the hour angle when the altitude angle is zero [46]. Sunrise and sunset time,

$$W_{sunrise} = \cos^{-1}.(-\tan(f).\tan(d)) \tag{2.9}$$

$$\omega_{sunset}' = \min\{ \ \omega_{ssunrise} \ , \ \cos^{-1}(-\tan(\phi - \beta)\tan\delta) \ \} \tag{2.10}$$

2.3.6. Zenith Angle (θ_z)

The angle between the vertical and the line to the sun, the angle of incidence of beam radiation on horizontal surface[48].

$$\cos\theta_z = \cos\phi \ \cos\delta \ \cos\omega + \sin\phi \ \sin\delta \tag{2.11}$$
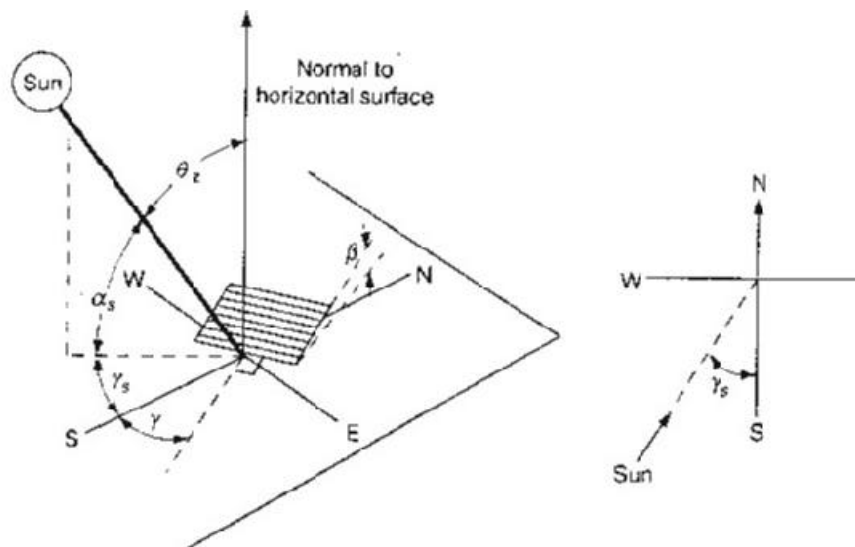
Figure 2.8 Zenith, Slope, Surface Azimuth Angle and Solar Azimuth Angle for a Tilted Surface [47].

2.3.7. Surface (γ) and Solar (γ_s) Azimuth Angle

Surface azimuth angle is deviation of the projection on a horizontal plane of the normal to the surface from the local meridian, with zero due south, east direction is negative and west is positive ; $-180^{\circ} \leq \gamma \leq 180^{\circ}$. Surface azimuth angle is shown in Figure 2.8. Solar azimuth angle is angular displacement from south of the projection of beam radiation on the horizontal plane [47], shown in Figure 2.8.

2.3.8. SolarAltitude Angle (α_s)

The angle between the horizontal and the line to the sun [47], shown in Figure 2.8.

2.3.9. Angle of Incidence (θ)

The angle between the beam radiation on a surface and the normal to that surface[47].

$$\text{Cos } \theta = \sin\delta \, \sin\phi \, \cos\beta - \sin\delta \, \cos\phi \, \sin\beta \, \cos\gamma + \cos\delta \, \cos\phi \, \cos\beta \, \cos\omega + \cos\delta \, \sin\phi \, \sin\beta \, \cos\gamma \, \cos\omega + \cos\delta \sin\beta \, \sin\gamma \, \sin\omega \qquad (2.12)$$

When surface azimuth angle $\gamma = 0$ Equation 2.12 becomes,

$$\text{Cos } \theta = \sin\delta \, \sin\phi \, \cos\beta - \sin\delta \, \cos\phi \, \sin\beta + \cos\delta \, \cos\phi \, \cos\beta \, \cos\omega + \cos\delta \, \sin\phi \, \sin\beta \, \cos\omega \qquad (2.13)$$

When $\theta = 90°$, the surface altitude angle β is equal to solar altitude angle α_s. Similarly the surface azimuth angle, γ is equal to solar azimuth angle, γ_s.

CHAPTER 3

WIND ENERGY

3.1. Wind Energy

Wind energy is rightfully an indirect form of solar energy since chiefly the uneven heating of the earth's crust induces wind by the sun. Power of energy coming from sun to earth is 10^{15} kW. It has been estimated that about 2 % of this radiation falling on the face of the earth is converted to kinetic energy in the atmosphere and that 30 % of this kinetic energy occurs in the lowest 1000 m of elevation. It is thus said that the total kinetic energy of the wind in this lowest kilometer, if harnessed, can satisfy considerable energy demand of the world [52,53].

Winds can be broadly classified as planetary and local. Planetary winds are caused by greater solar heating of the earth's surface near the equator than near the northern or southern poles. This causes warm tropical air to rise and flow through the upper atmosphere toward the poles and cold air from the poles to flow back to the equator nearer to the earth's surface. The direction of motion of planetary winds with respect to the earth is affected by the rotation of the earth. The western motion toward the equator and the eastern motion toward the poles result in large counterclockwise circulation of air around low-pressure areas in the northern hemisphere and clockwise circulation in the southern hemisphere [54].

Local winds are caused by two mechanisms. The first is differential heating of land and water. Solar insolation during the day is readily converted to sensible energy of the land surface and partly consumed in evaporating some of that water. The landmass becomes hotter than the water, which causes the air above land to heat up and become warmer than the air above water. The warmer lighter air above the land rises, and the cooler heavier air above the water moves in to replace it. This is the mechanism of shore breezes. At night, the direction of the breezes is reversed because the landmass cools more rapidly than the water. Hills and mountain sides cause the second mechanism of local winds. The air above the slopes heats up during the day and cools down at night, more rapidly than the air above the low lands. This causes heated air during the day to rise along the slopes and relatively cool heavy air to flow down at night.

Winds are very much influenced by the ground surface at altitudes up to 100 meters. The wind will be slowed down by the earth's surface roughness and obstacles. Wind speeds are affected by the friction against the surface of the earth. In general, the more pronounced the roughness of the earth's surface; the more the wind will be slowed down. Forests and large cities obviously slow the wind down considerably, while concrete runways in airports will only slow the wind down a little. Water surfaces are even smoother than concrete runways, and will have even less influence on the wind, while long grass and shrubs and bushes will slow the wind down considerably.

The roughness of the earth surface diminishes the velocity of the wind. With growing heights above ground level, the roughness has less effect and the velocity of the wind increases. Wind speed varies considerably with height above ground. This is called wind shear.

Sometimes still a power law is used for the description of the wind profile like:

$$V_b = V_a \left(\frac{h_b}{h_a} \right)^a \tag{3.1}$$

V_b= Wind speed at height h_b

V_a= Wind speed at height h_a

Value α is dependent on the roughness elements of the ground and is different from h_b. It is often stated that $\alpha = \frac{1}{7} = 0.14$ for open sites. There is increasing evidence that α varies with season and time through the day. In areas with a very uneven terrain surface, and behind obstacles such as buildings there is similarly created a lot of turbulence, with very irregular wind flows, often in whirls or vortexes in the neighborhood (Figure 3.1).
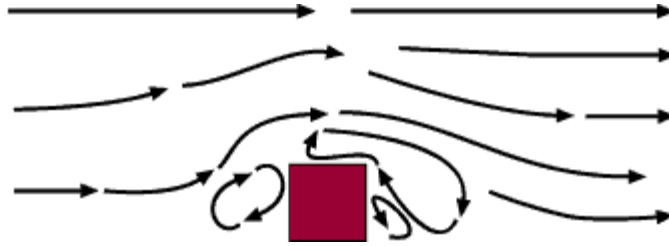
Figure 3.1 Turbulence Behind Obstacles [55].

A common way of siting wind turbines is to place them on hills or ridges overlooking the surrounding landscape. In particular, it is always an advantage to have as wide a view as possible in the prevailing wind direction in the area.

On hills, one may also experience that wind speeds are higher than in the surrounding area. Once again, this is due to the fact that the wind becomes compressed on the windy side of the hill, and once the air reaches the ridge it can expand again as its soars down into the low-pressure area on the lee side of the hill.

3.2. Power Extracted from the Wind

Wind turbines use the kinetic energy of the wind flow. Their rotors reduce the wind velocity from the undisturbed wind speed far in front of the rotor to a reduced air stream velocity behind the rotor. The difference in wind velocity is a measure for the extracted kinetic energy which turns the rotor connected electrical generator.

The total power of a wind stream is equal to the rate of the incoming kinetic energy of that stream, or

$$P_{tot} = \dot{m}\frac{V_1^2}{2} \qquad (3.2)$$

where,

P_{tot} = total power, W

$\dot{m}$ = mass-flow rate, kg/s

V_1 = incoming velocity m/s

The mass-flow rate is given by the continuity equation

$$\dot{m} = \rho A_1 V_1 \tag{3.3}$$

where,

ρ = incoming wind density, kg/m^3

A_1= rotor swept area, m^2

Then Equation 3.2 becomes as,

$$P_{tot} = \frac{1}{2} \rho A_1 V_1^{3} \tag{3.4}$$

Thus, the total power of a wind stream is directly proportional to its density, area, and the cube of its velocity (Figure 3.2).
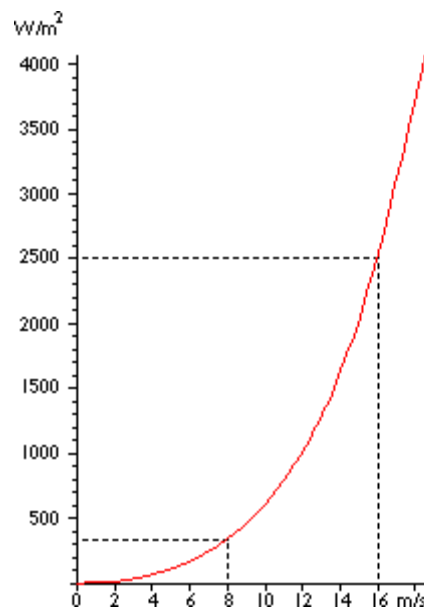
Figure 3.2 Wind Power is Proportional to Cube of Wind Speed [1].

Air density ρ is a function of height and meteorological condition. Wind speed increases with height, is affected by local topography, and varies greatly with time. We consider ρ constant with time and over the area of the air column. A typical value for ρ is 1.2 kg/m^3 at sea level, and useful power can be harnessed in moderate winds when V~10 m/s. In this condition P=600 W/m^2. In gale force conditions V~25 m/s, so P~10000 W/m^2.

Area A_1 is the rotor swept area. Areas A_0 and A_2 are upwind and downwind speed areas, respectively. A_0 and A_2 can be located experimentally for wind speed determination. Such measurement at A_1 is not possible because of the rotating blades.

The force or thrust on the turbine is the reduction in momentum per unit time from the air mass flow rate $\dot{m}$:

$$F = \dot{m}V_0 - \dot{m}V_2 \qquad (3.5)$$

This force is applied by an assumed uniform air flow of speed V_1. The power extracted by the turbine is

$$P_T = FV_1 = \dot{m}(V_0 - V_2)V_1 \qquad (3.6)$$

The loss in energy per unit time by that air stream is the power extracted from the wind:

$$P_W = \frac{1}{2}\dot{m}(V_0^2 - V_2^2) \qquad (3.7)$$

Equating (3.6) and (3.7)

$$\dot{m}(V_0 - V_2)V_1 = \frac{1}{2}\dot{m}(V_0^2 - V_2^2) = \frac{1}{2}(V_0 - V_2)(V_0 + V_2)V_1 \qquad (3.8)$$

Hence,

$$V_1 = \frac{V_0 + V_2}{2} \qquad (3.9)$$

Thus, according to the linear momentum theory, the air speed through the activator disk cannot be less than half the unperturbed wind speed.

Then, Equation (3.6) becomes as,

$$P_T = rA_1V_1^2(V_0 - V_2) \qquad (3.10)$$

substitution of V_2 from Equation (3.9) gives,

$$P_T = rA_1V_1^2[V_0 - (2V_1 - V_0)] = 2rA_1V_1^2(V_0 - V_1) \qquad (3.11)$$

The interference factor a is the fractional wind speed decrease at the turbine.

Thus,

$$a = \frac{V_0 - V_1}{V_0} \qquad (3.12)$$

$$V_1 = (1 - a)V_0 \qquad (3.13)$$

Equation (3.9) becomes as,

$$(1 - a) = \frac{V_0 + V_2}{2V_0} \qquad (3.14)$$

by using Equation (3.12) and (3.13) .

Equation (3.11) can be rewritten as,

$$P_T = 2rA_1(1 - a)^2V_0^2[V_0 - (1 - a)V_0] \qquad (3.15)$$

or

$$P_T = [\frac{1}{2}rA_1V_0^3][4a(1 - a)^2] \qquad (3.16)$$

If P_0 is considered as unperturbed wind, P_T can be written as,

$$P_T = C_pP_0 \qquad (3.17)$$

where, C_p is the power coefficient.

C_p is defined as portion of power extracted out of total wind power. C_p can be rewritten in terms of interference factor, a.

$$C_p = 4a(1-a)^2$$

(3.18)

The maximum value of C_p occurs when $a=1/3$;

$$C_{pmax} = \frac{16}{27} = \mathbf{0.59}$$

(3.19)

In other words, a wind turbine is capable of converting no more that 59 % of the total power of a wind to useful power. The criterion for maximum power extraction is called the Betz Criterion.
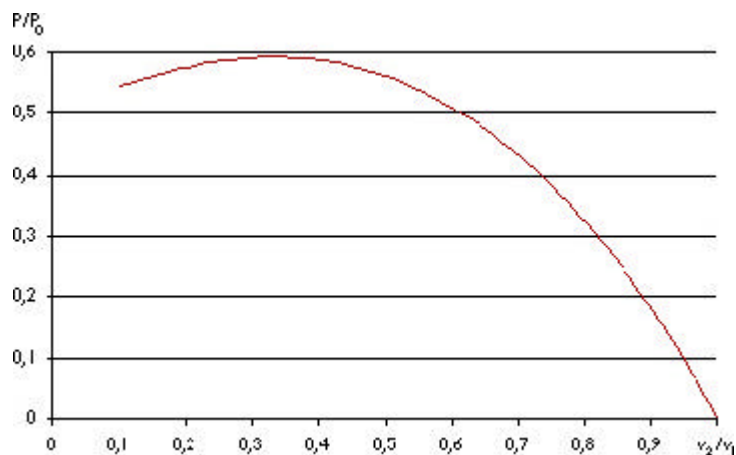
Figure 3.3 The Graph Shows "Betz Criterion"[1].

The power coefficient tells you how efficiently a turbine converts the energy in the wind to electricity. Very simply, we just divide the electrical power output by the wind energy input to measure how technically efficient a wind turbine is [1].

CHAPTER 4

HYBRID SYSTEM

Hybrid energy systems combine the use of two or more alternative power sources such as solar, wind, diesel, biofuels, hydrogen etc. Some hybrid systems incorporate a backup generator as well. Backup generators can be useful to supply the system an extra measure of protection for short periods, not as a primary power source, since fuel costs are much higher [56,57].

In a typical hybrid system, one power source is lower level while the other source is usually at higher levels. For example, when solar panels produce lower levels of energy, a wind generator may produce higher levels of energy on a cloudy and windy day. Contrary to this, on a bright cloudless day the solar panels will meet the most energy demand[58].

A typical hybrid system using photovoltaics and wind turbines may meet overall power needs better than either system could alone. This is true if the solar and wind resources are complementary. A typical hybrid system might have PV modules, a wind generator, a controller, and a battery and inverters as shown in Figure 4.1. These systems are backed up with a diesel generator set [58].
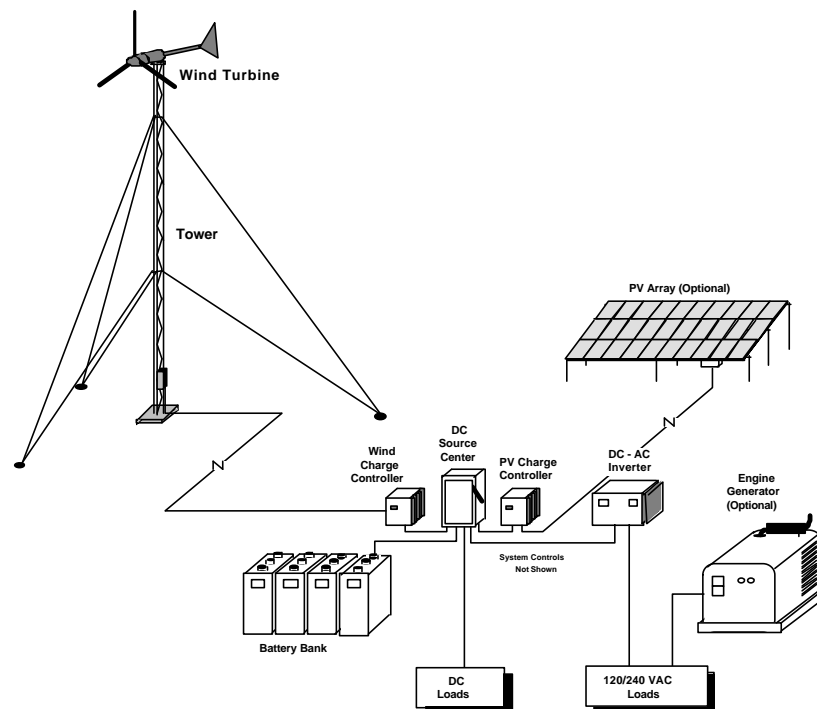
Figure 4.1 General Diagram of a Hybrid System [59].

Main application areas of the hybrid energy systems are:

- Remote settlements
- Telecomunication sites
- Light house
- Emergency warning systems

4.1. Components of a Wind / Solar Hybrid Energy System

4.1.1. Photovoltaic System

Photovoltaic system consist of solar cells. Solar cells are made from semiconductors and have much in common with other solid-state electronic devices, such as diodes, transistors and integrated circuits. For practical operation, solar cells are usually assembled into modules [41].

The photovoltaic effect was discovered by Becquerel in 1839, but the modern type of photovoltaic cell was not developed until 1954. In that year, Chapin, Fuller and Pearson devised the first effective solar cell [48].

When sunlight falls on the appropriate semiconductor material, the photons in the sunlight energise the valance electrons. Once a photon breaks a bond, an electron becomes free to move through the lattice. The absent electron leaves behind a vacancy, or a hole, that can also move through the lattice as electrons shuffle around it. In many respects, these holes behave as particles, similar to the electrons but are positively charged. The movement of the electrons and holes in opposite directions constitutes the electric current in the semiconductor [60].
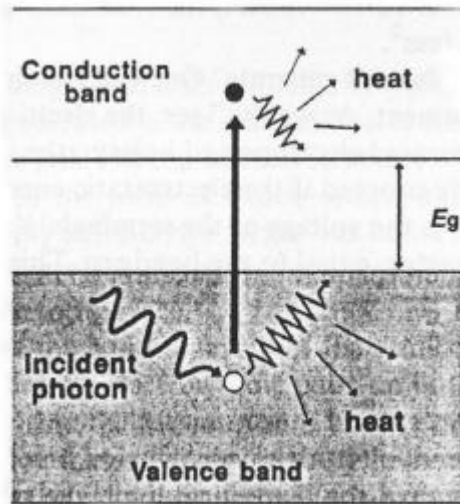
Figure 4.2 The Generation Of Electron-Hole Pairs By Light [41].

The two most important effects are insolation falling on it and temperature for the power (and current) output from a solar cell.

Effects of Temperature : This has an important effect on the power output from the cell. The most significant is the temperature dependence of the voltage which decrease with increasing temperature (its temperature coefficient is negative). The voltage decrease of a silicon cell is typically 2.3 mV per $^{\circ}$C. The temperature variation of the current or the fill factor are less pronounced, and are usually neglected in the PV system design [41].
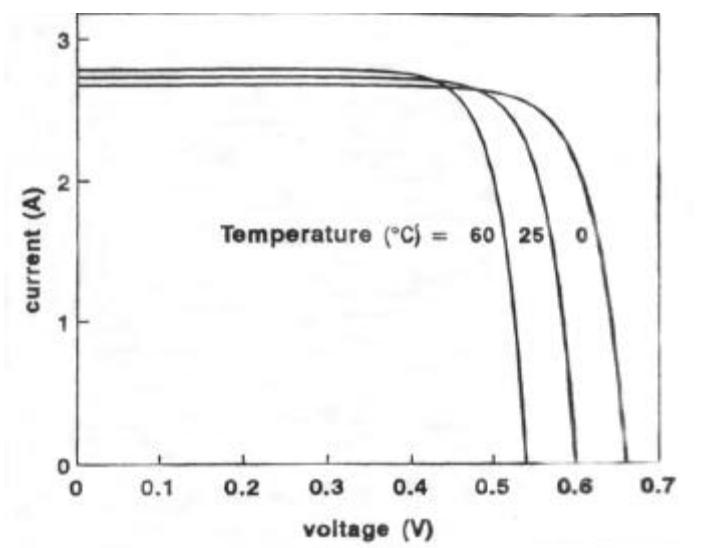
Figure 4.3 Temperature Dependence of the I-V Characteristic of a Solar Cell [41].

Effects of Insolation : The light –generated current is proportional to the flux of photons with above-bandgap energy. Increasing the irradiance inreases, in the same proportion, the photon flux which, in turn, generates a proportionely higher current. Therefore, the short circuit current of a solar cell is directly proportional to the irradiance. The voltage variation, is much smaller, and is usually neglected in practical applications[41].
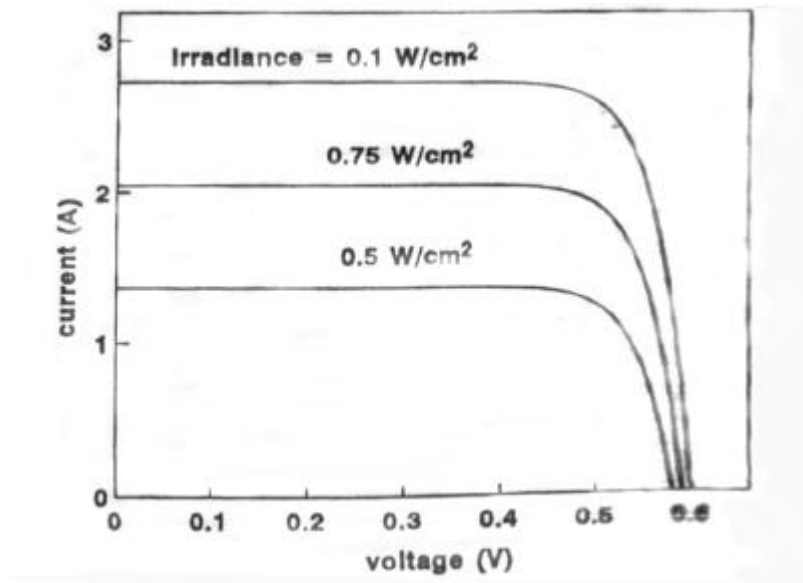
Figure 4.4 Irradiance Dependence of the I-V Characteristic of a Solar Cell [41].

When more power is required, modules can be connected together in series (i.e. positive to negative) in order to increase the voltage or in parallel (i.e. negative to negative, positive to positive) to increase the current outputs. This modular capability, so faciliating the installation of just the amount of power generation required, is one of the advantages of photovoltaic systems [60].

Series PV connection   Parallel PV connection
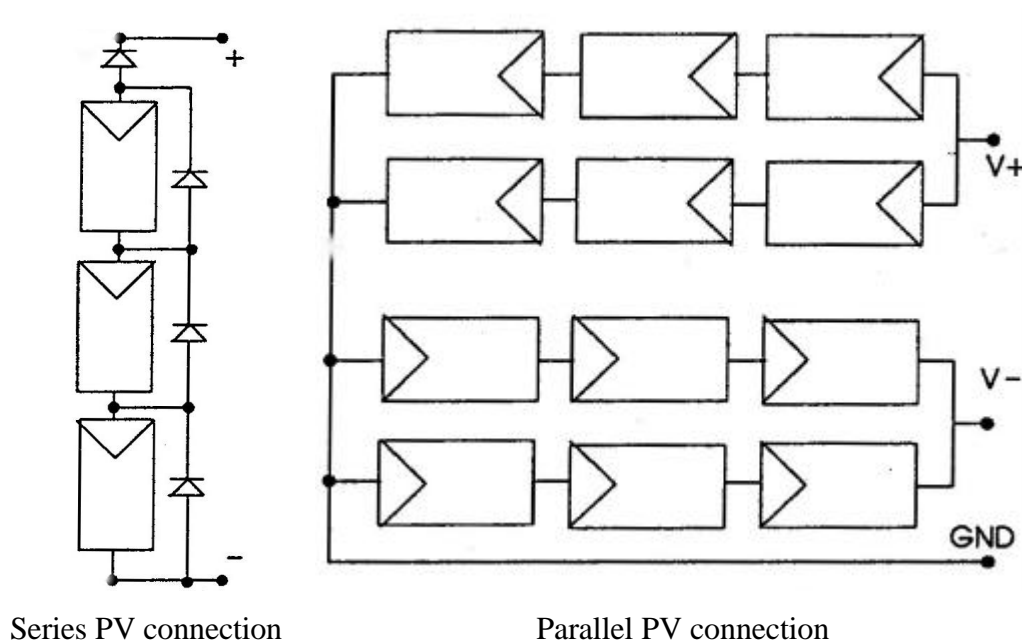
Figure 4.5 PV Connections (Series and Parallel) [41].

There are several material and techniques that have been used to manufacture solar cells ; single crystal, polycrystalline silicon, single-junction, multi-junction.

The followings are the advantages of PV systems:

- Access to the site: A well-designed photovoltaic system will operate unattended. The savings in labour costs and travel expenses can be significant.
- Fuel costs : For some remote locations,the transportation of fuel to the site can be a substantial contribution to the total cost of running the system. No fossil fuel is needed for the operation of a PV system.
- Maintenance : For photovoltaic systems, this is generally cheaper than for most alternative power sources.
- Durability : Photovoltaic modules have no moving parts, and degradation is slow.
- Modularity : A photovoltaic system can be easily expanded to suit future electric-power requirements.
- Environmental impact: Photovoltaic systems generate no harmfull effects to the environment as well as produce no noise.

The followings are the drawbacks of PV systems:

- Cost: At present PV system are expensive to purchase compared with other alternatives for providing electricity for the majority of applications.
- Efficiency: The conversion efficiencies are currently low and can be significantly reduced by the deposition of dust or other elements on the cover.
- High technology : The modules can be easily fractured (e.g. by children at play or even vandalism). They cannot be easily repaired onsite ; a replacement of the modules usually being necessary.
- Time dependent : The insolation is not always available. Night time electricity demand can be met only through battery storage or the other renewable energy conversion system in the hybrid system [60].

4.1.2. Wind System

Small wind energy systems can be used in connection with an electricity transmission and distribution system (called grid-connected systems), or in stand-alone applications that are not connected to the utility grid. A grid-connected wind turbine can reduce your consumption of utility-supplied electricity for lighting, appliances, and electric heat.

If the turbine cannot deliver the amount of energy you need, the utility makes up the difference. When the wind system produces more electricity than the household requires, the excess can be sold to the utility.

With the interconnections available today, switching takes place automatically. Stand-alone wind energy systems can be appropriate for homes, farms. That are far from the nearest utility lines [61,62].

All wind systems consist of a wind turbine, a tower, wiring.
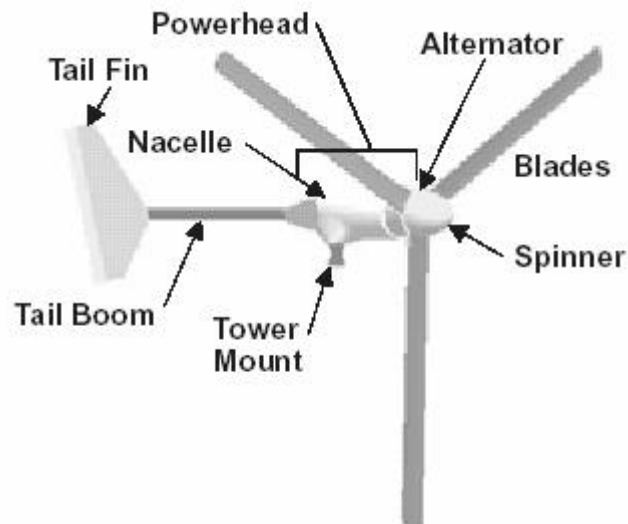
Figure 4.6 Wind Turbine [59].

Wind turbines consist of a rotor, a generator mounted on a frame, and a tail. Through the spinning blades, the rotor captures the kinetic energy of the wind and converts it into rotary motion to drive the generator. Rotors can have two or three blades, with three being more common.

The best indication of how much energy a turbine will produce is the diameter of the rotor, which determines its "swept area," or the quantity of wind intercepted by the turbine. The frame is the strong central axis bar onto which the rotor, generator, and tail are attached. The tail keeps the turbine facing into the wind.

A 1.5-kilowatt (kW) wind turbine will meet the needs of a home requiring 300 kilowatt-hours (kWh) per month, for a location with a 6.26 -meters-per-second annual average wind speed. The manufacturer will provide you with the expected annual energy output of the turbine as a function of annual average wind speed. The manufacturer will also provide information on the maximum wind speed in which the turbine is designed to operate safely.

Most turbines have automatic speed-governing systems to keep the rotor from spinning out of control in very high winds.

This information, along with your local wind speed distribution and your energy budget, is sufficient to allow you to specify turbine size[59]. Wind speeds increase with height in flat terrain, the turbine is mounted on a tower.

Generally speaking, the higher the tower, the more power the wind system can produce. The tower also raises the turbine above the air turbulence that can exist close to the ground. Experiments have shown that relatively small investments in increased tower height can yield very high rates of return in power production. There are two basic types of towers: self-supporting and guyed. Most home wind power systems use a guyed tower. Guyed-lattice towers are the least expensive option [59].

They consist of a simple, inexpensive framework of metal strips supported by guy cables and earth anchors. However, because the guy radius must be one-half to three-quarters of the tower height, guyed-lattice towers require enough space to accommodate them. Guyed towers can be hinged at the base so that they can be lowered to the ground for maintenance, repairs, or during hazardous weather such as hurricanes. Aluminum towers are prone to cracking and should be avoided [59].

There are two basic tower types for sensor mounting: tubular and lattice. For both, tilt-up, telescoping, and fixed versions are available. In addition, these versions may be either guyed or self-supporting. For most sites, tubular, tilt-up guyed types are recommended for their ease of installation (the tower can be assembled and sensors mounted and serviced at ground level), minimal ground preparation, and relative low cost.

Towers should:

- have an erected height sufficient to attain the highest measurement level,

- be able to withstand wind and ice loading extremes expected for the location,

- be structurally stable to minimize wind-induced vibration,

- have guy wires secured with the proper anchor type, which must match the site's soil conditions,

- be equipped with lightning protection measures including lightning rod, cable, and grounding rod,

- be secured against vandalism and unauthorized tower climbing,

- have all ground-level components clearly marked to avoid collision hazards,

- be protected against corrosion from environmental effects, including those found in marine environments [63,64].

4.1.3. Balance of he System

The "balance of system" components: controllers, inverters, and/or batteries. Stand-alone systems require batteries to store excess power generated for use when the wind is calm. They also need a charge controller to keep the batteries from overcharging. Deep-cycle batteries, such as those used to power golf carts, can discharge and recharge 80% of their capacity hundreds of times, which makes them a good option for remote renewable energy systems. Automotive batteries are shallow-cycle batteries and should not be used in renewable energy systems because of their short life in deep cycling operations [59].

In very small systems, direct current (DC) appliances operate directly off the batteries. If you want to use standard appliances that require conventional household alternating current (AC), however, you must install an inverter to convert DC electricity to AC.

Although the inverter slightly lowers the overall efficiency of the system, it allows the home to be wired for AC, a definite plus with lenders, electrical code officials, and future home buyers. For safety, batteries should be isolated from living areas and electronics because they contain corrosive and explosive substances. Lead-acid batteries also require protection from temperature extremes.

In grid-connected systems, the only additional equipment is a power conditioning unit (inverter) that makes the turbine output electrically compatible with the utility grid. No batteries are needed [59].

CHAPTER 5

MEASURING AND CALCULATION OF SOLAR ENERGY

5.1. Solar Data Measuring System Equipments

Solar radiation data are available in several forms. The following information about the radiation data is important in their understanding and use : whether they are instantaneous measurements (irradiance) or values integrated over some period of time (irradiation) which is hour and day. Two types of solar radiation data are widely available. The first is monthly average of daily total radiation on a horizontal surface. The second is hourly total radiation on a horizontal surface [47].

Measuring equipments for the different type of solar radiation ; Total (beam plus diffuse) solar radiation on horizontal surface is measured by a pyranometer. Beam (direct) solar radiation is measured by a pyrheliometer, but a pyrheliometer is required sun tracker system [47].

In this study, a pyranometer is mounted to measure total solar radiation and Liu-Jordan estimation method has been used to calculate beam and diffuse solar radiation (Equation 5.7).

5.1.1. Pyranometer

Instruments for measuring total (beam plus diffuse) radiation are referred to as pyranometers, and it is from these instruments that most of the available data on solar radiation are obtained. The dedectors for these instruments must have a response independent of wavelenght of radiation over the solar energy spectrum (short-wave is radiation originating from the sun, in the wavelenght range of 0.3 to 3 μm and long-wave radiation's wavelengths greater than 3 μm). Pyranometer is shown in Figure 5.1.

In radiation, they should have a response independent of the angle of incidence of the solar radiation. The dedectors of most pyranometers are covered with one or two hemispherical glass covers to protect them from wind and other extraneous effects; the covers must be very uniform in thickness so as not to cause uneven distribution of radiation on the detectors [47].

Figure 5.1 CM 11 Pyranometer [65].

A pyranometer produces a voltages from the thermopile detectors that is a function of the incident radiation. It is necessary to use a potentiometer to detect and record this output. Radiation data usually must be integrated over some period of time, such as an hour or a day.

Integration can be done by electronic integrators (data logger).It has been estimated that with careful use and reasonably frequent pyranometer calibration, radiation measurements should be good within ± 5 % ; integration errors would increase this number [47].

Two additional kind of measurements are made with pyranometers; measurements of diffuse radiation on horizontal surfaces and measurements of solar radiation on inclined surfaces. Measurements of solar radiation on inclined planes important in determining the input to solar collector.

 There is evidence that the calibration of pyranometers changes if the instrument is inclined to the horizontal. The reason for this appears to be changes in the convection patterns inside the glass dome, which changes the manner in which heat is transferred from the hot junction of the thermopiles to the cover and other parts of the instruments.

Measurements of diffuse radiation can be made with pyranometers by shading the instrument from beam radiation. This is usually done by means of shadow ring, as shown in Figure 5.2. The ring is used to allow continuous recording of diffuse radiation without the necessity of continuous positioning of smaller shading devices; adjustments need to be made for changing declination only.

Figure 5.2 Shadow Ring for CM 11 Pyranometer [65].

In this study, Kipp&Zonen CM 11 pyranometer is used. The pyranometer   CM 11 is designed for measuring the irradiance (radiant-flux, W/m^2) on a plane surface, which results from the direct solar radiation and from the diffuse radiation incident from the hemisphere above. Because the CM 11 exhibits no tilt dependence it can measure solar radiation on inclined surface as well [65].

Specifications of CM 11;

Wieving Angle   : 2π

Irradiance   : 0 - 1400 W / m^2

Sensitive   : 5.11*10^{-6} Volts per W/ m^2 (+/- 0.5 % at 20 ^{o}C and 500 W/m^2)

Expc. Signal Output   : 0 – 10 mV

Response time for 95 % response   : < 15 sec.

Figure 5.3 CM 11 Pyranometer at the Site.

The site is located a way from a shadow will not be cast on it any time and the site is chosen away from any obstruction over the azimuth range between earliest sunrise and latest sunset should have an elevation not exceeding 5°. This is important for an accurate measurement of the direct solar radiation. The diffuse solar radiation is less influenced by obstructions near the horizon (for example, by masts or exhaust pipes). Hot exhaust gas will produce radiation in spectral range of the CM 11 pyranometer. The pyranometer is located far from light-coloured walls or other objects likely to reflect sunlight onto it [47,65].

5.1.2. Data Logger

The data logger is a 10 channel datalogger that functions both as a data logging device and a multichannel, autoranging meter. The LI-1000 datalogger is also well suited to measure low impedance voltage sensors such as thermocouples, and sensors with a pulsed output .A wide variety of other sensors for environmental and industrial test and measurement can also be measured with the LI-1000 datalogger.

In this study, a 10 channel LI-1000 Data Logger is used and two current input channels are located on the two sealed BNC connectors so the equipment above are not used. Data is output through an RS-232C interface cable, maximum, minimum reading [66].

Figure 5.4 LI-1000 Data Logger at the Site[66].

Six alkaline "d" call battaries are installed in the LI-1000 at the factory. Battery life varies with instrument configuration and temperature.

At 25 ^{o}C Battery Life ;

- 8 channels, 1 to 24 hour periods

60 second sampling : 10 months

5 second sampling : 1 month

- 1 channel, 1 to 24 hour periods

60 second sampling : 12 months

- 1 channel,10 minute periods :55 days

- 8 channels,10 minute periods :30 days

When there is 10 % of battery life left, the word "^{L}$_O$ " is displayed to indicate the battery voltage is low. If operation is continued, automatic shutoff will occur when the battery voltage drops to 5.8 volts. After automatic shutoff, the memory is maintained by the remaining power in the batteries. For long term indoor monitoring applications the AC adapter can be used to provide continuous power [66].

The LI-1000 datalogger configured as LIGHT sensor channel. Configuration in LOG Mode : Logging period 10 minutes and the sampling period 5 second.The datalogger store a mean value hich is sum divided by the number of samples. Treshold is 1 W/m^2 ,the treshold parameter is very useful for radiation sensors.

By setting the treshold at a low value, the LI-1000 can be made to collect data during the day when the sensor output is high, but not at night when sensor output is below the treshold value. Min/max value of radiation is stored during day. Range is set the autorange. Multiplier of the data logger is calculated from calibration constant of the pyranometer; mult = $1/5.11*10^{-3}$(mV). Where $5.11*10^{-3}$ is pyranometer calibration constant in mV.

5.2. Measurements of Total Solar Radiation on a Horizontal Surface

These data are available from ESRA (European Solar Radiation Atlas), the Izmir city appears in ESRA stations list and its WMO (World Meteorological Organisation) number is 17220, latitude is 38.43 degree, longitude is 27.17 degree, elevation from the sea level is 25 meters. And these data are also available from the Turkish State Meteorological Sevice (DMI) and the General Directorate of Electrical Power Resources Survey and Development Administration (EIEI) .

In this study , solar radiation data for the IZTECH campus area are measured by a Kipp&Zonen (CM11) pyranometer which is mounted at the top of the Mechanical Engineering Laboratories Building shown in Figure 5.3. Measured total solar radiation data on horizontal surface is shown in Table 5.1.

Table 5.1 Monthly Average of Daily Total Solar Radiation on Horizontal Surface

Months	$\underline{H}$ (Measured) (Wh/ m2-day)	$\underline{H}$ (Measured) (MJ / m2-day)
January	1742.8	6.3
February	2646.6	9.5
March	3419.8	12.3
April	4234.9	15.2
May	6192.0	22.3
June	6816.8	24.5
July	6662.4	24.0
August	5839.1	21.0
September	3916.2	14.1
October	3334.9	12.0
November	1798.8	6.5
December	1375.9	5.0
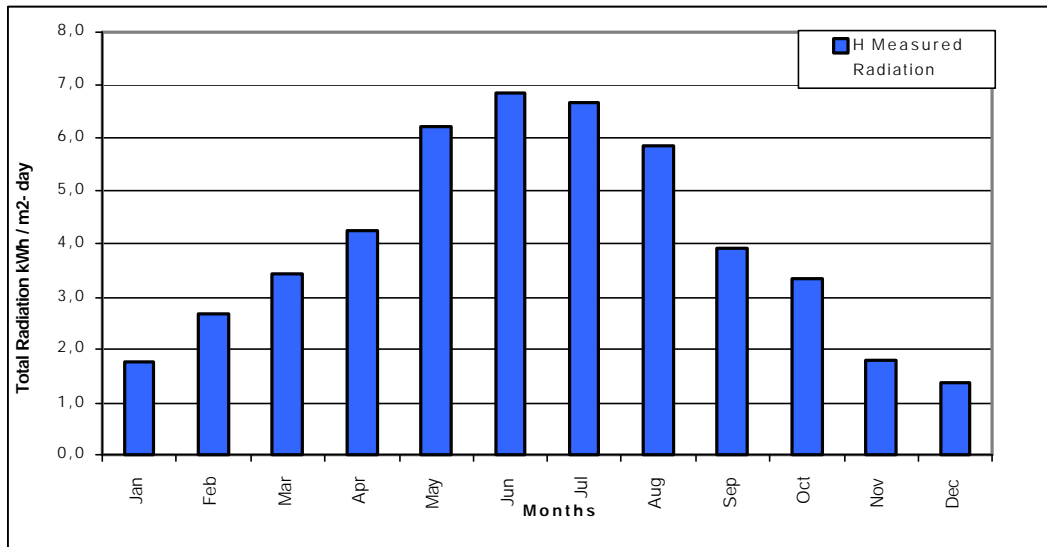
Figure 5.5 Monthly Average of Daily Total Solar Radiation on Horizontal Surface

5.3. Calculation of Total Solar Radiation on a Inclined Surface

Radiation on tilted surfaces can be calculated by using data measured on horizontal surfaces. If the diffuse sky radiation is uniformly distributed over the sky dome, the amount of this radiation that falls on a surface depends on how much of the sky the surface sees [20,47,67,68].
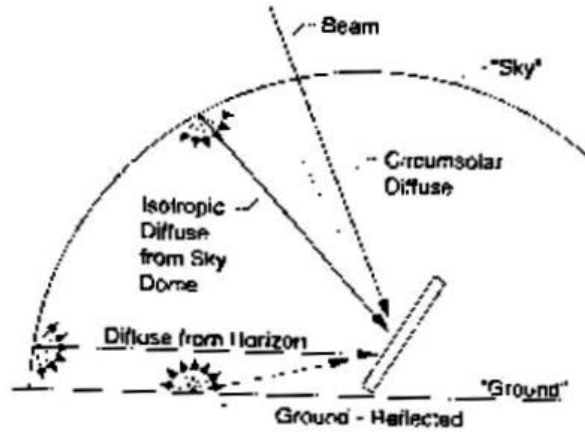
Figure 5.6 Beam, Diffuse, and Ground-Reflected Radiation On Tilted Surface [47].

$$H_T = H_b \ R_B + H_d \ (1+ \cos \beta) / 2 + (H_b + H_d) \ \boldsymbol{r} \ (1 - \cos \beta) / 2 \qquad (5.1)$$

where, H_T is the total solar radiation on tilted surface

$$H = H_b + H_d \qquad (5.2)$$

where, H is the total solar radiation on a horizontal surface which is sum of the horizotal beam and diffuse radiation (measured data).

$$R_B = H_T / H_o = \cos \theta / \cos \theta \ z \qquad (5.3)$$

where, R_B is the beam radiation tilt factor.

$\underline{R_B} = [\cos (\phi - \beta) \cos \delta \sin \omega_{sunset}{}' + (\pi/180) \ \omega_s{}' \sin (\phi-\beta) \sin \delta] / [\cos \phi \cos \delta \sin \omega_{sunset}{}' + (\pi/180) \ \omega_s \sin \phi \sin \delta]$ \qquad (5.4)

$$R = (H_T / H) = (H_b / H)R_B + (H_d / H) (1+ \cos \beta) / 2 + \boldsymbol{r} (1 - \cos \beta) / 2 \quad (5.5)$$

where, R is the total radiation tilted factor

$$\underline{R} = (\underline{H_T} / \underline{H}) = [1 - (\underline{H_d} / \underline{H})]\underline{R_B} + (\underline{H_d} / \underline{H}) (1 + \cos \beta)/2 + \boldsymbol{r} (1 - \cos \beta)/2 \quad (5.6)$$

Table 5.2 Solar Reflectance Values for 15 Characteristic Surfaces [43].

SURFACES	AVERAGE REFLECTIVITY (r)
Snow(freshly fallen or withice film)	0.75
Watersurfaces (relatively large incidence angles)	0.07
Sils(clay, loam ,etc.)	0.14
Earths roads	0.04
Coniferous forest (winter)	0.07
Forests in autumn, ripe field crop, plants	0.26
Weathered blacktop	0.10
Weathered concrete	0.22
Dead leaves	0.30
Dry grass	0.20
Green grass	0.26
Bituminous and gravel roof	0.13
Crushed rock surface	0.20
Building surfaces, dark (red brick, dark paints, etc.)	0.27
Building surfaces, light (light brick, light paints, etc.)	0.60

A simplified method for the estimation of monthly average of daily total radiation incident on tilted surface has been developed by Liu-Jordan. Their correlation expresses the diffuse-total radiation ratio for a horizontal surface in terms of the monthly average clearness index K_T

$$H_d / H = 1.39 - 4.027\ K_T + 5.531\ K_T^{\,2} - 3.1008\ K_T^{\,3} \qquad (5.7)$$

where, H_d is monthly average of daily diffuse solar radiation on horizontal surface.

$$K_T = H / H_o \qquad (5.8)$$

where, H is monthly average of daily total radiation on horizontal surface (measured data) given in Table 5.1 and H_o monthly average daily total extraterrestrial radiation on horizontal surface is shown Figure A.1(in Appendix A).

Monthly average of daily total solar radiation on tilted surface ($S = H_T$) caculated by using Mathlab software. and these data are given in Table 5.3

Table 5.3 Monthly Average of Daily Total Solar Radiation on Tilted Surface.

Months	$S = \underline{H}_T$ (Wh / m2)	$\underline{H}_T$ (MJ / m2)
January	2694.4	97
February	3694.4	13.3
March	4027.8	14.5
April	4250.0	15.3
May	5528.0	19.9
June	5722.2	20.6
July	5694.4	20.5
August	5555.6	20.0
September	4305.5	15.5
October	4500.0	16.2
November	2700.0	9.6
December	2138.0	7.7
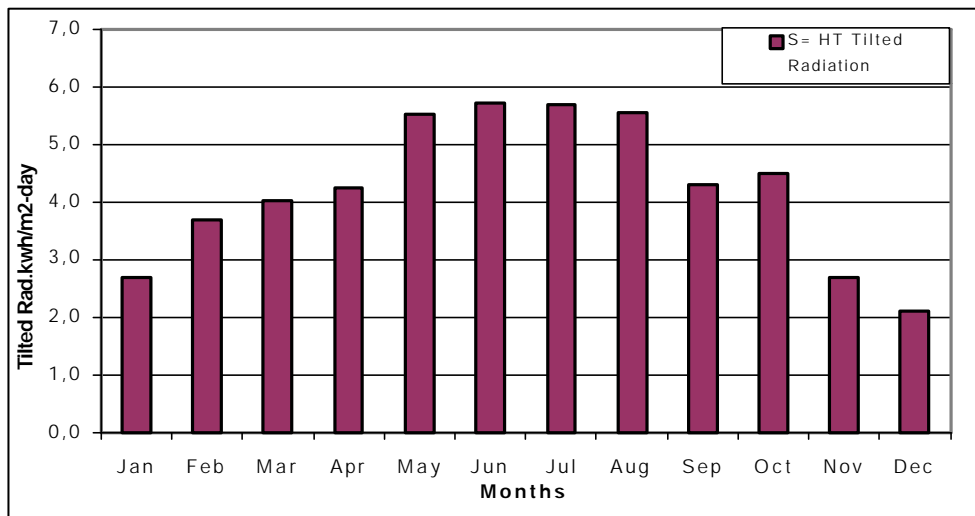
Figure 5.7 Monthly Average of Daily Total Solar Radiation on Tilted Surface.

CHAPTER 6

MEASURING AND CALCULATION OF WIND ENERGY

6.1. Wind Speed

In order to measure wind speed, two types of anemometers are used : cup anemometer and propeller anemometer. The wind turbine captures the wind's kinetic energy in a rotor consisting of two or more blades mechanically coupled to an electrical generator. The turbine is mounted on a tall tower to enhance the energy capture. Numerous wind turbines are installed at one site to build a wind farm of the desired power production capacity. Obviously, sites with steady high wind produce more energy over the year[62].

Cup anemometer is an instrument consists of a cup assembly (three or four cups) centrally connected to a vertical shaft for rotation. At least one cup always faces the oncoming wind. The aerodynamic shape of the cups converts wind pressure force to rotational torque. The cup rotation is nearly linearly proportional to the wind speed over a specified range. A transducer in the anemometer converts this rotational movement into an electrical signal, which is sent through a wire to a data logger. The data logger then uses known multiplier (or slope) and offset (or intercept) constants to calculate the actual wind speed.

Propeller anemometer is an instrument consists of a propeller mounted on a horizontal shaft that is oriented into the wind through the use of a tail vane. The propeller anemometer also generates an electrical signal proportional to wind speed.

Although the two sensor types differ somewhat in their responsiveness to wind speed fluctuations, there is no clear advantage of one type over the other. In practice, the cup type is most commonly used for resource assessment.

In this study, two Ammonit brand three cups "Classic" model anemometer are being used. They are mounted on IZTECH mast at 10 m and at 30 m. Their technical data are as following: Measurement range 0.3 ... 50 m/s, Accuracy ± 2 % of measurement value or ± 0.3 m/s, Resolution 0.05 m/s, Distance constant 5 m, Max. wind load 60 m/s, Ambient temperature -35 °C ... + 80 °C, Power supply 4 - 18 V DC - approx. 0.35 mA, Heating 24 V AC/DC max. 20 W, Weight without cable 1 kg [69].

Figure 6.1 Anemometer at Site.

6.2. Wind Direction

A wind vane is used to measure wind direction. The most familiar type uses a fin connected to a vertical shaft. The vane constantly seeks a position of force equilibrium by aligning itself into the wind. Most wind vanes use a potentiometer type transducer that outputs an electrical signal is transmitted via wire to a data logger and relates the vane's position to a known reference point.

Therefore, the alignment of the wind vane to a specified reference point is important. The data logger provides a known voltage across the entire potentiometer element and measures the voltage where the wiper arm contacts a conductive element. The ratio between these two voltages determines the position of the wind vane. This signal is interpreted by the data logger system, which uses the ratio (a known multiplier) and the offset (a known correction for any misalignment to the standard reference point) to calculate the actual wind direction. Electrically the linear potentiometer element does not cover a full 360°. This "open" area is the deadband of the wind vane. When the wiper arm is in this area, the output signal is random. Some manufacturers compensate for the deadband in their data logger software to prevent random signals. Therefore, the deadband area should not be aligned into or near the prevailing wind direction. When choosing a wind vane, the same selection criteria as for the anemometer are applicable.

Particular attention to the size of the open deadband area of the potentiometer should be paid; this should not exceed 8°. The resolution of the wind vane is also important. Some divide a complete 360° rotation into 16°, 22.5° segments. This resolution is too coarse for optimizing the layout of a wind turbine array.

In this study, Ammonit brand "Classic" type wind vane is chosen because of its simple design and low maintenance requirements. With the help of a potentiometer the physical property is converted into an analogue resistor output signal. At zero the transducer has to pass the „north transition" between the margins of zero and 2 kohm. Its technical data are as following: Measurement range 0 ... 360° without north gap, Accuracy ± 2°, Resolution 1°, Damping coefficient > 0.3, Max. wind load 60 m/s, Ambient temperature -35 °C ... + 80 °C, Power supply max. 50 V, max. 100 mA, Heating 24 V AC/DC max. 20 W, Weight without cable 1.5 kg [70].

Figure 6.2 Wind Vane at the Site**.**

6.3. Air Temperature

A typical ambient air temperature sensor is composed of three parts: the transducer, an interface device, and a radiation shield. The transducer contains a material element (usually nickel of platinum) with a relationship between its resistance and temperature. Thermistors, resistance thermal detectors (RTDs), and semiconductors are common element types recommended for use. The resistance value is measured by the data logger (or an interface device), which uses a known equation to calculate the actual air temperature.

The transducer is housed within a radiation shield to protect it from direct solar radiation. In this study, Ammonit "temp-humidityprobe" series xPC model is selected because of its compact size and stick version sensor with fixed connected cable. The temperature measurement is made by Pt100-resistor. The signal is available directly (4-wire-connection) or as an analogue output as well. The relative humidity is measured by a capacitive sensing element and the value will be placed at the output as analogue signal. For protection against rain and direct radiation a weather and radiation shield is mounted. Humidity has no influence on the energy analysis, but the readings can help to asses the danger of freezing at the location.

Technical data of temperature probe is as following:

Temperature range -30 .. +70 °C, Accuracy ± 0.2 K, Additional error ± 0.004 %/K (<10 °C, >40 °C), Resolution 0.1 °C, Response time 5 min. Measurement principle Pt100 - 1/3 DIN, Output signal 4-wire-connection or 0..1 V, Ambient temperature -40 °C ... + 80 °C Operation supply 9 - 30 V DC - approx. 1 mA Protection (sensor/electronic) IP 30 / IP 65 Weight Sensor without cable 0.350 kg, shield 1 kg [63].

Technical data of humidity probe is as following:

Humidity range 0 .. 100 % r.H., Accuracy ±2 % r.H., Additional error ± < 0.1 %/K (<10 °C, >40 °C) Resolution 1 % r.H. Response time 5 min., Measurement principle capacitive, Output signal 0..1 V, Operation supply 9 - 30 V DC - approx. 1 mA Protection (sensor/electronic) IP 30 / IP 65 [63].
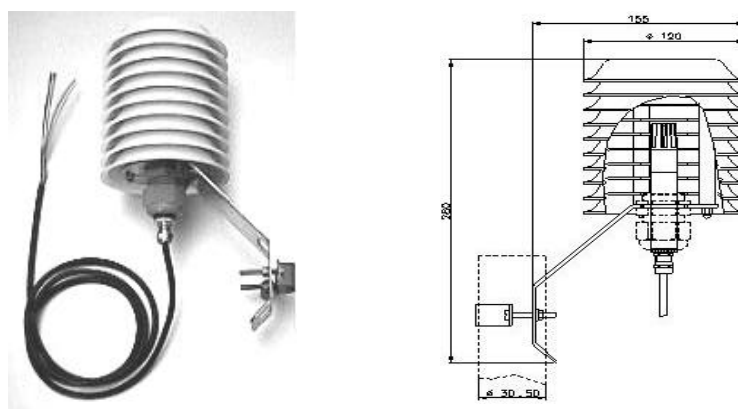
Figure 6.3 Ammonit thermo/hygro probe [71].

6.4. Collecting Wind Data

6.4.1. Data Logger

Data loggers come in a variety of types and have evolved from simple strip chart recorders to integrated electronic on-board cards for personal computers. Many manufacturers offer complete data logging systems that include peripheral storage and data transfer devices. Data loggers can be grouped by their method of data transfer, either in-field or remote. Those that feature remote phone modem or cellular phone data transfer capabilities allow you to obtain and inspect stored data without making frequent site visits.

The data logger should be electronic and compatible with the sensor types, number of sensors, measurement parameters, and desired sampling and recording intervals. It should be mounted in non-corrosive, water-tight, lockable electrical enclosure to protect itself and peripheral equipment from the environment and vandalism. It should also:

- be capable of storing data values in a serial format with corresponding time and date stamps,
- contribute negligible errors to the signals received from the sensors,
- have an internal data storage capacity of at least 40 days,
- operate in the same environmental extremes,
- offer retrievable data storage media.

Their drawback is that they need a continuous power source to retain data. Data loggers that incorporate the use of internal backup batteries or use non-volatile memory are available. They are preferred because data cannot be lost due to low battery voltage.

There are two commonly used formats for recording and storing data, ring memory and fill and stop [72].

- Ring Memory: In this format, data archiving is continuous. However, once the available memory is filled to capacity, the newest data record is written over the oldest. The data set must be retrieved before the memory capacity of the storage device is reached.

- Fill and Stop Memory: In this configuration, once the memory is filled to capacity, no additional data are archived. This effectively stops the data logging process until more memory becomes available. The device must be replaced or downloaded and erased before the data logger can archive new data.

WICOM-CM wind computer from Ammonit is mounted on IZTECH mast. It is capable to calculate three wind speeds and one wind direction and is equipped with additional inputs for a barometer, a thermometer, and a hygrometer. This additional data is recorded just, as the other measurement values, as mean, maximum and minimum values and as standard deviation in measurement series. Air temperature and air pressure are needed to calculate air density. Temperature and humidity give information about the weather conditions, e.g. if your site is in danger of frost.

Programming and data retrieval of Ammonit data loggers is done with serial RS232 interface (PC software is included). The RS232 interface also allows operation of remote data transfer for easy data control and retrieval. The current operating condition of the measurement equipment can be controlled through the display.

Figure 6.4 Ammonit Wicom CM data logger [72].

6.4.2. Data Transfer Equipment

Data are typically retrieved and transferred to a computer either manually or remotely. Manual data transfer method requires site visits to transfer data.

Typically this involves two steps: (1) remove and replace the current storage device (e.g., data card) or transfer data directly to a laptop computer; and (2) upload the data to a central computer in an office.

The advantage of the manual method is that it promotes a visual on-site inspection of the equipment. Disadvantages include additional data handling steps (thus increasing potential data loss) and frequent site visits.

Remote transfer requires a telecommunication system to link the in-field data logger to the central computer. The communications system may incorporate direct wire cabling, modems, phone lines, cellular phone equipment, or RF telemetry equipment, or some combination thereof. An advantage of this method is that you can retrieve and inspect data more frequently than you can conduct site visits. This allows you to promptly identify and resolve site problems. Disadvantages include the cost and time required to purchase and install the equipment. This may prove worthwhile in the long term if data monitoring problems can be spotted early and quickly remedied.

IZTECH mast was also equipped with Siemens M29 GSM-system, which makes it possible to make a remote contact with the station by computer or mobile phone. The GSM-system includes: the modem, an antenna and an activation unit, so that the modem can be switched on and off at programmed times.

"CALLaLOG" which is a Windows application program is being used for remote and manual data transfer and configuration of wind computer. All parameter settings also can be transferred to logger. In online operation it is possible to observe the current measurement values.

WicomCM data logger has a connection for an external DC supply which is being used for battery which is charged by a solar power module.

6.4.3. Power Supplies

All electronic data logger systems require a main power source that is sized to meet the total power requirements of the system. A backup power supply should be included to minimize chances of data loss caused by power failure. The backup system should be designed with the objective of saving the stored data. This can be accomplished by shutting down peripheral devices (modems, cellular telephones, and other data transfer equipment) at a designated low voltage level, or isolating a particular power source that is dedicated to protecting the data.

Most systems offer a variety of battery options including long-life lithium batteries or lead acid cells with various charging options (AC or solar powered). Examples of power supplies are presented below.

AC power (through a power transformer) should be used as the direct source of system power only if a battery backup is available. In this case, AC power should be used to trickle charge a storage battery that provides power to the data logger.

Lead Acid Battery: Lead acid storage battery is the preferred power source. It withstands repeated discharge and recharge cycles without significantly affecting the energy storage capacity of the battery. It also offers a margin of safety over a wet acid battery, Because the acid is contained in a gel and cannot be easily spilled.

Solar Power : The solar recharge option is a convenient way to recharge a lead acid battery when AC power is unavailable. The solar panel must supply enough wattage to recharge the battery and maintain system power during extended periods of low solar conditions (i.e., winter months). As a precaution, the battery should be sized to provide at least a week of reserve capacity to power the entire system without recharging. Be sure that the solar panel is reverse bias protected with a diode to prevent power drain from the battery at night. In addition, the solar panel must include a voltage regulator to supply a voltage compatible with the battery and to prevent overcharging.

6.5. Mast Erected on the Campus Area

IZTECH mast is 30 m tall tubular tower, which was erected in July 2000. It has two Ammonit "Classic" series anemometers which are 10 m and at 30 m and a Ammonit "Classic" series wind vane at 30 m. Temperature, humidity and atmospheric pressure data are obtained from Ammonit "xPC" series temp&humidity probe and Ammonit pressure gauge, which are all mounted on the mast. Ammonit "WicomCM" type wind computer is connected with all sensors on the mast to collect data in time series. Wind computer's power is supplied from external battery charged by solar panel or from its two batteries inside in emergency cases[62].

Mast is also equipped with Siemens M29 GSM modem system, which is used by wind computer to achieve remote connections for changing configurations and data transferring. Detailed technical data about all equipment are given in previous sections.

Figure 6.5 IZTECH Mast at Site.

6.5.1. Collected Wind Data from IZTECH Mast

Mean wind speed at 10 and 30 meter are measured at IZTECH mast, which is 380 meter height from sea level, is given in Table 6.1 below.

Table 6.1 Measured Mean Wind Speed at IZTECH Mast.

Mean Wind Speed (m/s)			
Months	**10 meter**	**30 meter**	**h (from sea)**
January	6.5	7.6	380
February	6.6	7.8	380
March	7.0	8.0	380
April	6.7	7.5	380
May	6.2	6.4	380
June	7.3	8.3	380
July	6.6	7.6	380
August	7.2	8.4	380
September	5.7	6.6	380
October	6.6	7.8	380
November	6.3	7.4	380
December	7.7	9.2	380
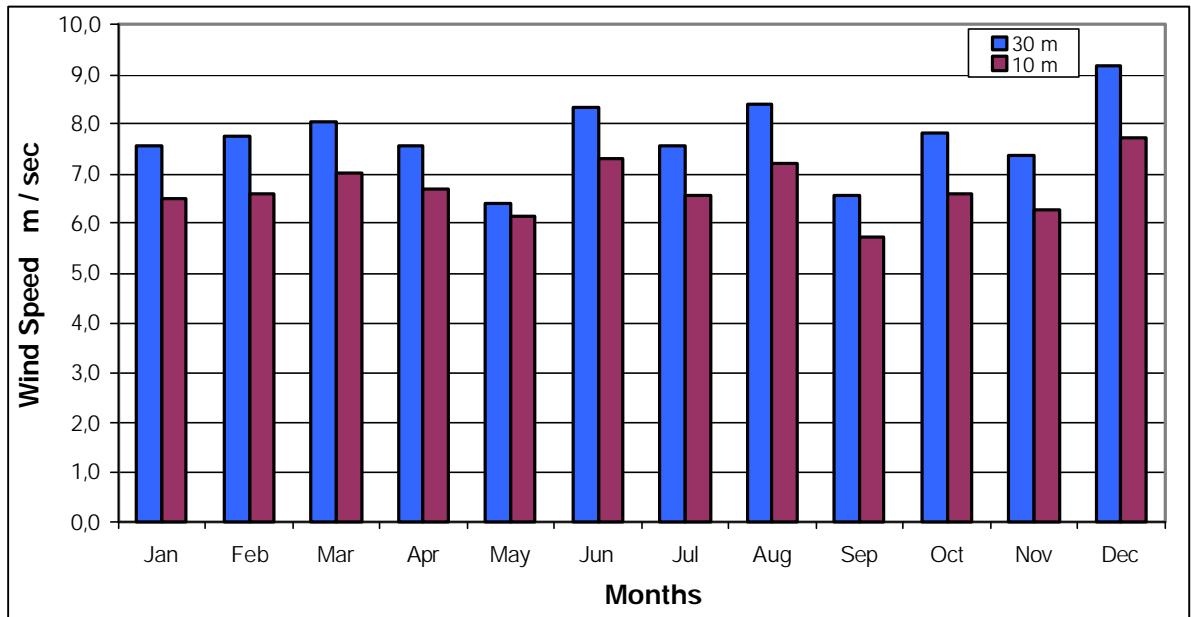
Figure 6.6 Mean Wind Speed at 380 meter.

6.6. Wind Energy Calculation

The total power of wind is equal to ;

$$P_{tot} = \frac{1}{2} \rho A V_i^3 \qquad (6.2)$$

P_{tot} = total power, W

V_i = incoming velocity, m/s

ρ = incoming wind density, kg/m^3

A = cross- sectional area of stream, m^2

Monthly average of daily total wind energy per square meter *(W)* calculated by Equation (6.3) is seen below ;

$$W = \frac{1}{2} \rho V_i^3 * D \qquad (6.3)$$

where,

D = Duration of 1 day

Table 6.2 Monthly Average of Daily Total Wind Energy at 380 meter.

Months	Wind Energy (W) kWh / m² - day	
	10 m	**30 m**
January	2.5	4.0
February	2.6	4.3
March	3.2	4.8
April	2.8	3.9
May	2.1	2.4
June	3.6	5.3
July	2.6	4.0
August	3.5	5.5
September	1.7	2.6
October	2.6	4.4
November	2.3	3.7
December	4.3	7.1
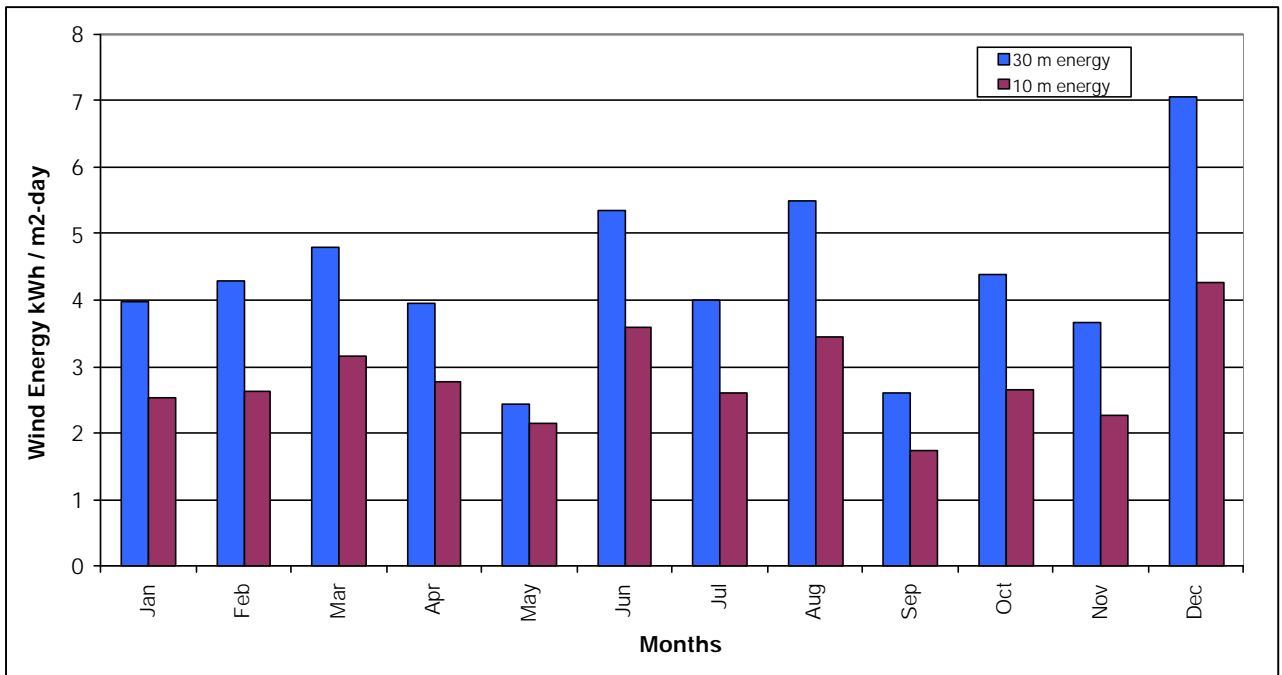
Figure 6.7 Monthly Average of Daily Total Wind Energy at 380 meter.

CHAPTER 7

SIZE OPTIMIZATION OF A HYBRID ENERGY SYSTEM

If the hybrid systems are designed well, they provide a reliable service and, free from the need for fuel supply, can even operate unattended for extended periods of time. Unlike conventional generators, however, these systems use fluctuating and finite energy resources, and this feature must be reflected in the system design. An important aspect of this design is sizing.

7.1. Optimization Procedure

Optimization helps to find the answer that yields the best result the one that attains the highest profit, output, or happiness, or the one that achieves the lowest cost, waste, or discomfort. Often these problems involve making the most efficient use of resources including money, time, machinery, staff, inventory, and more. On the other hand, in an optimization problem one seeks to maximize or minimize a specific quantity, called the objective, which depends on a finite number of input variables. These variables may be independent of one another, or they may be related through one or more constrains. A mathematical program is an optimization problem in which the objective and constraints are given as mathematical functions and functional relationship [73];

$$\text{Object to (Optimize) :} \quad z = f(x_1, x_2, ... x_n) \tag{7.1}$$

$$
\begin{aligned}
\text{Subject to} \quad &: \ g_1(x_1, x_2, .. x_n) && \leq && b_1 \\
& g_2(x_1, x_2, .. x_n) \ \ \} \ \{=\} \ \ \{ && b_2 && \tag{7.2} \\
& .... && \geq && ... \\
& g_m(x_1, x_2, .. x_n) && && b_m
\end{aligned}
$$

Each of the m constraint relationships in Equation (7.1) involves one of the three signs $\leq$, $=$, $\geq$. Optimization problems are often classified as linear and nonlinear ;

7.2. The Linear Programming

Linear programming (LP) is a tool for solving optimization problems. In 1947, George Dantzig developed an efficient method, the simplex algorithm, for solving linear programming; the word programming does not refer here to computer pogramming; problems (also called LP). Since development of simplex algorithm, LP has been used to solve optimization problems in industries as drive as banking, education, forestry, petroleum, and trucking. A mathematical model is linear if $f(x_1, x_2, ... x_n)$ and each $g_i(x_1, x_2, ... x_n)$ (i=1,2, ...m) are linear. Any other mathematical model is nonlinear [73,74,75].

$$z = f(x_1, x_2, ... x_n) = c_1 x_1 + c_2 x_2 + ... + c_n x_n \qquad (7.3)$$

$$g_i(x_1, x_2, ... x_n) = a_{i1} x_1 + a_{i2} x_2 + ... + a_{in} x_n \qquad (7.4)$$

Certain symbols are commonly used to denote the various components of a linear programming model. These symbols are listed below, along with their interpretation for the general problem of allocating resources to activities.

z = value of overall measure of performance.

x_j = level of activity j (j= 1,2,...,n).

c_j = increase in z that would result from each unit increase in level of activity j.

b_i = amount of resource i that is available for allocation to activities (for $i=1,2,..,m$)

a_{ij} = amount of resource i consumed by each unit of activity j.

The model poses the problem in terms of making decision about the level of the activities, so $x_1, x_2, ... x_n$ are called the *decision variables*. The values of c_j, b_i and a_{ij} (for $i=1,2,...m$ and $j= 1,2,...,n$) are the *input constant* (known constant) for the model. The c_j, b_i and a_{ij} are also referred to as the parameters of the model [75].

In any linear programming problem, the decision marker wants to maximize (usually revenue or profit) or minimize (usually cost) some function of the decision variables. The function to be maximized or minimized is called the *objective function.* The coefficient of a variable in the objective function called *objective function coefficient* of the variable. For example, objective function coefficient for x_j is c_j. The restrictions normally are referred to as *constraints*. The $x_j \geq 0$ restrictions are called nonnegativity constraints (or nonnegativity conditions). Similarly, the first m constraints (those with a function of all the variables $a_{i1}x_1 + a_{i2}x_2 + ... + a_{in}x_n$ on the left-hand side) are sometimes called *functional constraints* (or structural constraints) [75].

A linear programming problem (LP) is an optimization problem for which we do the following :

1. We attempt to maximize or minimize a linear function of the decision variables. The function that is to be maximized or minimized is called the objective function.

2. The values of the decision variables must satisfy a set of constraints. Each constraint must be a linear equation or linear inequality.

3. A sign restriction is associated with each variable. For any variable x_j, the sign restriction specifies either that x_j, must be nonnegative ($x_j \geq 0$) or that x_j may be unrestricted in sign [76].

7.2.1. Solution Methods of Linear Programming Problems

There is three different method for the solution of linear programming problems;

- Graphical Method
- Simplex Method
- Matrix Method

Also, some computer programs can be used for optimization problems. LINDO is one of them.

In this study, graphical method have been used to solve the linear programming problems. Therefore, only the graphical method is explained. On the other hand LINDO has been used to compare with graphical solution.

7.2.2. Graphical Method

This procedure involves constructing a two-dimensional graph with x_1 and x_2 as the axes. The first step is to identify the values of (x_1 , x_2) that are permitted by the restrictions. This is done by drawing each line that borders the range of permissible values for one restriction. To begin, note that the nonnegativity restrictions $x_1 \geq 0$ and $x_2 \geq 0$ require (x_1 , x_2) to lie on the positive side of axes [75].

First, need to show how to graph the set of points satisfying a linear inequality involving only two variables. Consider a linear inequality constraint of the form $f(x_1, x_2) \geq b$ or $f(x_1, x_2) \leq b$. In general, it can be shown that in two dimensions, the set of points satisfying a linear inequality includes the points on the line $f(x_1, x_2) = b$ defining the inequality plus all points on one side of the line according to a maximization or a minimization problem. Now, the points, which are fail to satisfy, are eliminated. After these points are eliminated from consideration, the feasible region are left. Having identified the feasible region, now search for the optimal solution, but optimal solution changes according to maximization or minimization problem [76] ;

Here, any specification of values for the decision variables (x_1, x_2,... x_n) is called a solution, regardless of whether it is a desirable or even an allowable choice. Different types of solutions are then identified by using an appropriate adjective. A *feasible solution* is a solution for which all the contraints are satisfied. An *infeasible solution* is a solution for which at least one contraint is violated. The *feasible region* is the collection of all feasible solutions. Given that there are feasible solutions, the goal of linear programming is to find a best feasible solution, as measured by the value of the objective function in the model. An *optimal solution* is a feasible solution that has the most favorable value of the objective function. The *most favorable value* is the largest value if the objective function is to be maximized, whereas it is the smallest value if the objective function is to be minimized [75].

- Maximization Problem :

$$\text{Maximize} \quad : z = c_1 x_1 + c_2 x_2 + \dots + c_n x_n \tag{7.5}$$

Subject to the restrictions :

$$a_{11} x_1 + a_{12} x_2 + \dots + a_{1n} x_n \leq b_1$$
$$a_{21} x_1 + a_{22} x_2 + \dots + a_{2n} x_n \leq b_2 \tag{7.6}$$
$$.$$
$$a_{m1} x_1 + a_{m2} x_2 + \dots + a_{mn} x_n \leq b_m$$

For a maximization problem ; to find the optimal solution, which will be the point in the feasible region with largest value of objective function (z), must be need to graph a line on which all points have same z value. In max problem, such a line is called an *isoprofit line.* To draw an isoprofit line, choose any point in the feasible region and calculate its z value, all isoprofit lines have the same slope. This means that once one isoprofit line is drawn and all the other isoprofit lines can be found by moving parallel to the isoprofit line have been drawn. It is now clear how to find the optimal solution to a two-variable LP. After the isoprofit line have been drawn, generate other isoprofit lines by moving parallel to the drawn isoprofit line in a direction that increase z . After a while, the isoprofit lines will no longer intersect the feasible region. The last isoprofit line intersecting (touching) the feasible region defines the largest z value of any point in the feasible region and indicates the optimal solution to the LP.

- Minimization Problem :

$$\text{Minimize} \quad : z = c_1 x_1 + c_2 x_2 + \dots + c_n x_n \tag{7.7}$$

Subject to the restrictions :

$$a_{11} x_1 + a_{12} x_2 + \dots + a_{1n} x_n \geq b_1$$
$$a_{21} x_1 + a_{22} x_2 + \dots + a_{2n} x_n \geq b_2 \tag{7.8}$$
$$.$$
$$a_{m1} x_1 + a_{m2} x_2 + \dots + a_{mn} x_n \geq b_m$$

For a minimization problem ; to find the optimal solution, which will be the point in the feasible region with smallest value of objective function (z), must be need to graph a line on which all points have same z value. In min problem, such a line is called an *isocost line*. To draw an isocost line, choose any point in the feasible region and calculate its z value, all isocost lines have the same slope. This means that once one isocost line is drawn and all the other isocost lines can be found by moving parallel to the isocost line have been drawn. It is now clear how to find the optimal solution to a two-variable LP. After the isocost line have been drawn, generate other isocost lines by moving parallel to the drawn isocost line in a direction that decrease z. After a while, the isocost lines will no longer intersect the feasible region. The last point in the feasible region that intersects (touching) an isocost line will be the point in the feasible region having the smallest z value. This point is the optimal solution of the LP [75,76].

Any problem having multiple optimal solutions will have an infinite number of them, each with the same optimal value of the objective function. Another possibility is that a problem has no optimal solutions. This occurs only if (1) it has no feasible solutions or (2) the constraints do not prevent improving the value of the objective function (z) indefinitely in the favorable direction (positive or negative) [75].

7.3. Hybrid System Sizing

A procedure has been developed by Tomas Markvart, which determines the sizes of the PV array and wind turbine in a PV/wind energy hybrid system. Using the measured avarage monthly values of solar and wind energy at a given location, the method employs a simple graphical construction, which is explaine above, to determine the optimum configuration of the two generators that satisfies the energy demand of the user throughout the year.by a simple graphical procedure.

The sizes of the two generators a_s and a_w will be defined in terms of the conversion efficiency multiplied by the effective area of the generator. Thus, for the PV array ;

$$a_s = h * A_s \tag{7.9}$$

Where, h is the module efficiency and A_s is the array area. This definition coincides with the usual peak power rating of the array: if A_s is measured in m^2 , a_s is numerically equal to the peak power in Wp.

For the wind generator we define ;

$$a_w = Cp * (\boldsymbol{p} * r^2) \qquad (7.10)$$

where, Cp is the (dimensionless) power coefficient, and r is the radius of the rotor. Equation (7.9) and Equation (7.10) provide a conveniently symmetric description of the two generators. The energy resources will be described by the average daily energy incident on a unit area.

For the solar energy ($S = H_T$), the required value refers to the inclined surface of the modules, which is calculated from the measured data for a horizontal surface, is given in Table 4.3. The wind energy (W) is calculated by Equation (6.3) and W is given in Table 6.4 . If we assume that the average daily demand d as a function of the time in the year is known, we can readily write down the condition that the monthly average daily energy supply satisfies the demand :

$$W * a_w + S * a_s \geq d \qquad (7.11)$$

The simple formalism based on Inequality (7.11) can be used to develop a realistic sizing procedure for the hybrid generator. Seasonal analysis can be done, includes only two season, summer and winter [77] ;

$$W_{summer} * a_w + S_{summer} * a_s \geq d_{summer} \qquad (7.12)$$

$$W_{winter} * a_w + S_{winter} * a_s \geq d_{winter} \qquad (7.13)$$

The summer- winter analysis can be refined further by specifying the demand and resource data at more frequent intervals. The graphical representation in the $a_s - a_w$ plane provides a convenient description of all solutions of Inequality (7.11) but the infinity of values is clearly of little practical relevance : within the feasibility range we need to specify one system which is optimal.

7.4. IZTECH Campus Area Case Study

According to, graphical solution methods ; hybrid system optimization problem is a linear programming model. Since, the object function and each subject function are linear. And it is a typical minimization problem, because of, minimum cost.

Object function (Optimum) :

Minimum $\rightarrow$ Hybrid Generator Cost : $C_h = C_s * a_s + C_w * a_w$ (7.14)

Subject to restriction   :

$$W_{Jan} * a_w + S_{Jan} * a_s \geq d_{Jan} \tag{7.15}$$

$$W_{Feb} * a_w + S_{Feb} * a_s \geq d_{Feb} \tag{7.16}$$

$$W_{Dec} * a_w + S_{Dec} * a_s \geq d_{Dec} \tag{7.17}$$

$$W_{Dec} * a_w + S_{Dec} * a_s \geq d_{Dec} \tag{7.18}$$

$$W_{Dec} * a_w + S_{Dec} * a_s \geq d_{Dec} \tag{7.19}$$

$$W_{Dec} * a_w + S_{Dec} * a_s \geq d_{Dec} \tag{7.20}$$

$$W_{Dec} * a_w + S_{Dec} * a_s \geq d_{Dec} \tag{7.21}$$

$$W_{Dec} * a_w + S_{Dec} * a_s \geq d_{Dec} \tag{7.22}$$

$$W_{Dec} * a_w + S_{Dec} * a_s \geq d_{Dec} \tag{7.23}$$

$$W_{Dec} * a_w + S_{Dec} * a_s \geq d_{Dec} \tag{7.24}$$

$$W_{Dec} * a_w + S_{Dec} * a_s \geq d_{Dec} \tag{7.25}$$

$$W_{Dec} * a_w + S_{Dec} * a_s \geq d_{Dec} \tag{7.26}$$

where, a_s and a_w are the decision variables, C_s, C_w , $W_{Jan}, W_{Feb}, .., W_{Dec}$, S_{Jan}, $S_{Feb}, ..., S_{Dec}$, $d_{Jan}, d_{Feb}, ..., d_{Dec}$ are the known input constant for the linear hybrid system model. C_s and C_w represent the costs of solar and wind energy generators and C_h is cost of hybrid system per unit power of the output rating.

Constraints   : Nonnegativity constraints $a_s \geq 0$ and $a_w \geq 0$

In this study, an off-grid operated GSM base station's electricity demand is suggested to be met by a wind/solar hybrid energy system. This GSM base station is

assumed to be mounted at 380 m hight where the IZTECH mast is mounted. An identical grid operated GSM base station which has been located on the campus area was taken into consideration in terms of energy demand. The electricity consumption of the GSM base station was taken from the IZTECH Construction Department. The electricty demand, solar and wind energy potentials and unit cost values are shown in Table 7.1.

Figure 7.1 GSM base station

The hybrid combination of wind/solar energy system can provide a continuous source of energy due to the comlete each other discontinuity. To complete at each other about discontinuity of the wind and solar energy can be seen below in Figure 7.2.
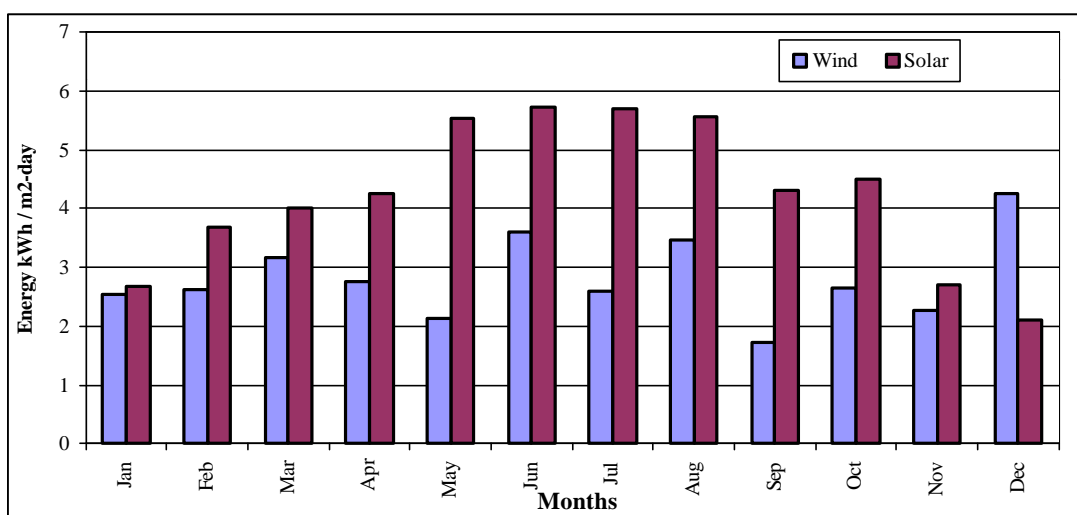
Figure 7.2 The Monthly Average of Daily Total Solar and Wind Energy at IZTECH (Solar energy data are for 38^0 panel inclination).

Table 7.1 GSM System Demand, Wind / Solar Energy, Cost of Wind and solar Generators [60,78,79,80].

Months	Demand d (kWh/day)	Solar Energy S (kWh/m²-day)	Wind Energy W (kWh/m²-day)	Wind Generator Cost C_w ($ / W)	Solar Generator Cost C_s ($ / Wp)
January	15.3	2.7	2.5	3	5.8
February	17.7	3.7	2.6	3	5.8
March	14.5	4.0	3.2	3	5.8
April	18.5	4.3	2.8	3	5.8
May	19.2	5.5	2.1	3	5.8
June	25.2	5.7	3.6	3	5.8
July	22.5	5.7	2.6	3	5.8
August	32.4	5.6	3.5	3	5.8
September	18.3	4.3	1.7	3	5.8
October	22.5	4.5	2.6	3	5.8
November	18	2.7	2.3	3	5.8
December	20.9	2.1	4.3	3	5.8

Thus, subject to restriction for every month ;

$$2.7 * a_s + 2.5 * a_w \geq 15.3 \qquad \text{(January)}$$

$$3.7 * a_s + 2.6 * a_w \geq 17.7 \qquad \text{(February)}$$

$$4.0 * a_s + 3.2 * a_w \geq 14.5 \qquad \text{(March)}$$

$$4.3 * a_s + 2.8 * a_w \geq 18.5 \qquad \text{(April)}$$

$$5.5 * a_s + 2.1 * a_w \geq 19.2 \qquad \text{(May)}$$

$$5.7 * a_s + 3.6 * a_w \geq 25.2 \qquad \text{(June)}$$

$$5.7 * a_s + 2.6 * a_w \geq 22.5 \qquad \text{(July)}$$

$$5.6 * a_s + 3.5 * a_w \geq 32.4 \qquad \text{(August)}$$

$$4.3 * a_s + 1.7 * a_w \geq 18.3 \qquad \text{(September)}$$

$$4.5 * a_s + 2.6 * a_w \geq 22.5 \qquad \text{(October)}$$

$$2.7 * a_s + 2.3 * a_w \geq 18 \qquad \text{(November)}$$

$$2.1 * a_s + 4.3 * a_w \geq 20.9 \qquad \text{(December)}$$

Min generator cost equations are the same for each month ;

$$\text{Minimum Hybrid Cost} \quad : \quad C_h = 3 * a_w + 5.8 * a_s \qquad (7.27)$$
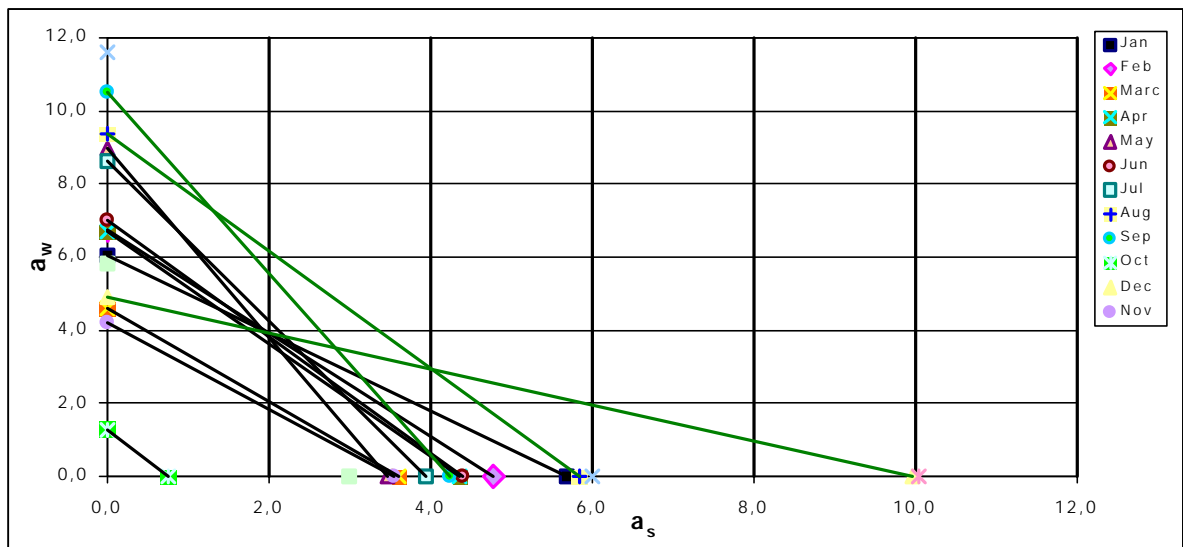
Figure 7.3 Graph Solution of Hybrid System.

Feasible region for the wind and solar hybrid system is upper region of the green lines. For the minimization problem. which will be the point in the feasible region with

smallest value of objective function (hybrid generator cost) must be need to graph isocost line. The "peak-watt" (Wp) price was used as a fixed economic parameter [78]. These isocost lines, which are blue, can be seen in Figure 7.3.
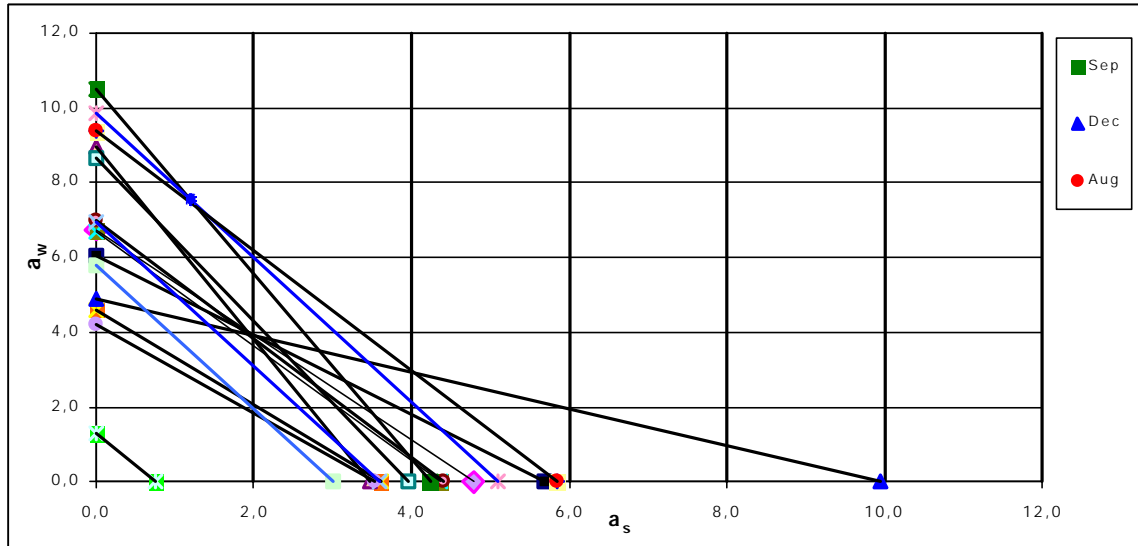
Figure 7.4 Isocostline for Optimum Solution

The point which isocost line first intersect the feasible region is optimum point of the hybrid system. The blue point in the graph near the feasible region that intersects an isocost line. Intersection of August and September line have the smallest *cost* . This point is the optimal solution of the hybrid energy system. This point correspondences to value of 7.3 at y axis and to value of 1.3 at x axis of the Graph Solution.On the other hand the same optimization of hybrid system can be done by LINDO program.

Where, a_s and a_w values of optimum hybrid system are 1.3 and 7.3 respectively. These values are exactly the same values gained by using Graph Solution.

7.4.1. Hybrid System Sizing

The sizes of the two generators are defined according to a_s and a_w values obtained by using "Graph Solution" and "LINDO" software.

$$A_s = a_s / \eta = 1.3 / 0.11 = 12 m^2$$

Where η is the module efficiency. This efficiency is assumed as 11 % [60,78]. A_s is array area (m^2). For the wind generator ;

$$A_w = a_w / C_p = 7.3 / 0.35 = 21 \ m^2$$

Where, Cp is power efficiency. This efficiency is assumed as 35 % [81,82].

For the 21 m^2 swept area of the wind turbine a generator, with 5 kW nominal power, was selected. Electricity supply for each month of this turbine is shown in Table 7.2. For the 12 m^2 total array areas 18 PV panels, each has 75 W nominal power, are selected for the hybrid energy system. Electricity supply for each month of these panels are shown in Table 7.2. More detailed tecnical specification for wind turbine. PV panel and other hybrid system equipment are given in Appendicies.

A wind and solar hybrid system equipments are ;

- 18 mono crystal PV each has 75 watt and 12 volts. 4.4 amp. PV array can be connected parallel or serial. For the case study, PV voltage output is 48 volts, therefore, PV panels are connected parallel and serial groups.
- One small wind generator with 5 kW and 5m blade diameter. Turbine mast is 10 meter height. Turbine has 48 volts output.
- And 1 charge regulator which has 60 ampers current and 48 volts voltage.
- Battery is chosen for no-sun and no-wind period. If no-sun and no-wind period is accured. Batteries can give electricity to the utility for example 1 days period. For the GSM system max load is 32.4 kWh /day.

- Battaries can be chosen 12 volts and 200 Ah. their total power is 2.4 kWh. Batteries recharge only 70 % of the charge value [78,81,83]. So total battery capacity is 42 kWh. 18 battaries are required to storage energy. Battaries can be connected parallel or series.

- One inverter with 3500 watt and 48 VDC-230 VAC. Inverter converts the DC current into the AC. Inverter was choosen according to the load.
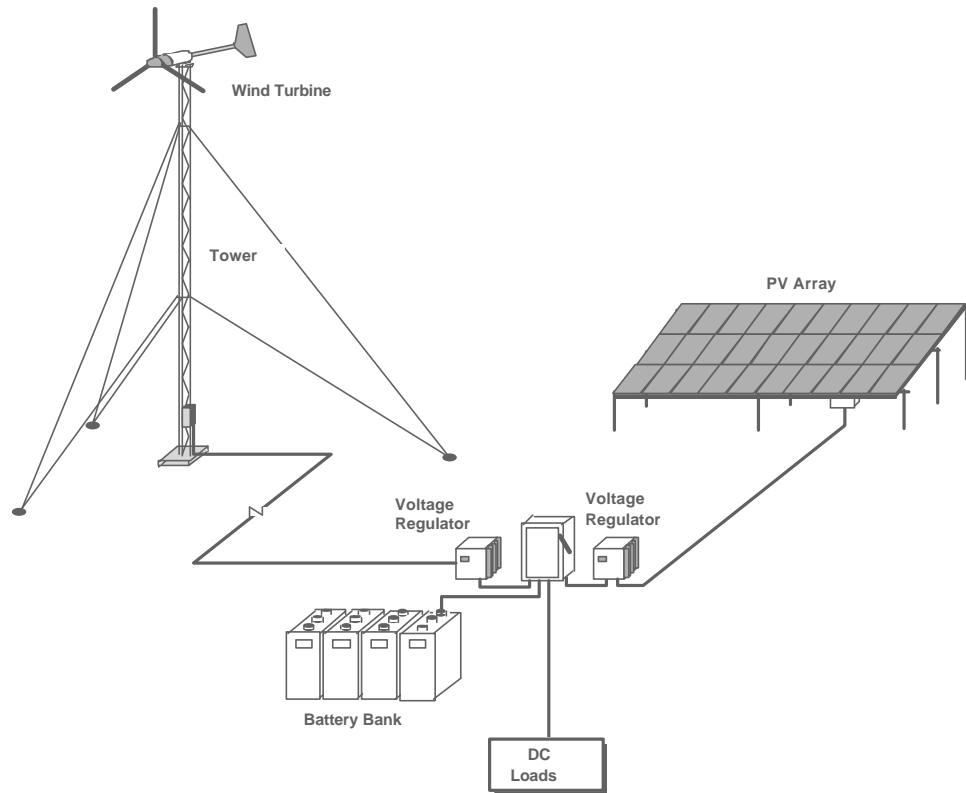
Figure 7.5 Hybrid System Equipments [59].

Table 7.2 Electricity Demand and Supply.

Months	Wind 5 kW (21 m^2) kWh/day	PV 18*75 W (12 m^2) kWh/ day	Hybrid kWh/ day	GSM Load kWh/day	Differences (Hybrid- GSM) kWh/day
January	17.8	3.6	22	15.3	6.9
February	18.3	4.9	24	17.7	6.4
March	22.1	5.3	29	14.5	14.0
April	19.4	5.6	26	18.5	7.4
May	15.0	7.3	23	19.2	3.8
June	25.2	7.6	34	25.2	8.8
July	18.2	7.5	27	22.5	4.1
August	24.2	7.3	33	32.4	0.3
September	12.1	5.7	18	18.3	0.2
October	18.5	5.9	25	22.5	2.9
November	15.9	3.6	20	18	2.3
December	29.8	2.8	34	20.9	13.1
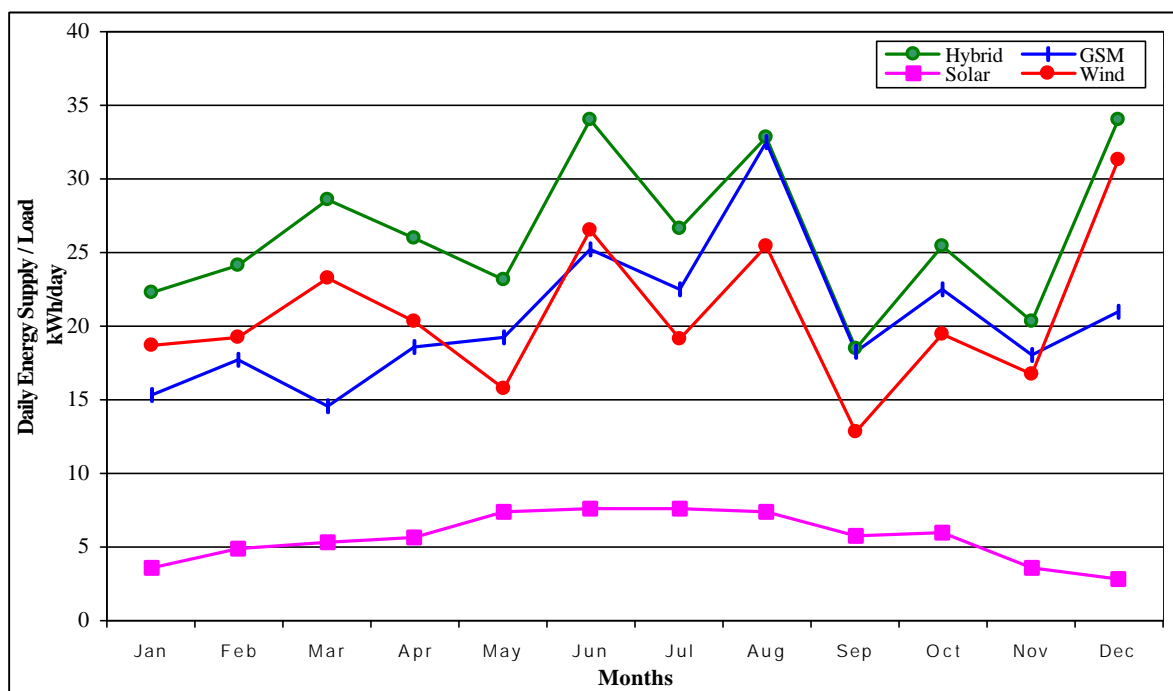
Figure 7.6 Monthly Variation of Supply and Load.

CHAPTER 8

DISCUSSION AND CONCLUSION

Hybrid energy systems on the basis of solar and wind generators in combination with a battery storage are now proven technologies for the supply of small electrical loads, espacially, isolated and remote locations which far from the grid lines.

In this thesis, A procedure for optimizing the size of a hybrid energy system contains photovoltaic panels and wind generator backed-up by batteries has been studied. The procedure was applied for the sizing of wind/solar hybrid system that is considered to supply a load of a GSM base station located on the campus area of Izmir Institute of Technology. For this specific system considered in this thesis, the results showed a clear benefit of exploiting the complementarity of both solar and wind energy resources.

The meteorological data for a given location were collected for a year between 01.01.2002. and 31.12.2002. For the characteristics of the wind, very detailed statistical analysis has been done by using a special software called WindPRO. This study indicated a great wind power capacity of the area.

Solar radiation data have been measured and analyzed in the form of total radiation on horizontal surface. The measured solar data have been corresponded to same period with wind measurements. Total radiation values on horizontal surface have been transferred to total radiation on tilted surface, due to the mounting of photovoltaics.

The solution of optimization was displayed in a graphical form. Sizes of solar and wind components have been shown as a cartesian coordinates. Same analysis have been done by using LINDO software and the same optimum values have been obtained.

It has been indicated that the hybrid system solution is more appropriate one than the PV array or wind turbine alone. Because energy supplied by hybrid system can be overlapped more closely to the specific load compared with seperate operation of PV array and wind turbine.

REFERENCES

[1]   J. TWIDEL, T. WEIR, *"Renewable Energy Resources"*, E&FN SPON, London, 1996.

[2]   A. SAYIGH, "Renewable Energy the way forward", *Applied Energy,* 1999, Vol. 64, pp. 15-30.

[3]   G.T. WRIXON, M.E. ROONEY, W. PALZ, "Renewable Energy 2000", *Springer Verlag*, 1993, Berlin, Germany.

[4]   A.DEMIRBAS, "Biomass and the other renewable and sustainable energy options for Turkey in the twenty-first century", *Energy Sources,* 2001, Vol.23, pp. 177-187.

[5]   Turkish Scientific and Technologic Research Committee (TUBITAK)-Turkish Technology Development Committee (TTGV), Science-Technology-Industry Discussion Platform, *"Energy Technologies Policies Study Group Report",* 1998, Ankara, Turkey.

[6]   World Energy Council Turkish National Committee, WEC-TNC, *"Energy Report 1"*, 1998, Ankara, Turkey.

[7]   E. TASDEMIROGLU, R. SEVER, "Estimation of monthly average daily, horizontal diffuse radiation in Turkey", *Energy,* 1991, Vol. 16(4), pp. 787-790.

[8]   IT.TOGRUL, E. ONAT, "A study for estimating solar radiation in Elazig using geographical and meteorological data", *Energy Conversation and Management*, 1999, Vol. 40, pp. 1577-1584.

[9]   K. KAYGUSUZ, "The comparison of measured and calculated solar radiations in Trabzon, Turkey", *Energy Sources*, 1999, Vol. 21, pp. 347-353.

[10]   M. TIRIS, C. TIRIS, I.E. TURE, "Correlations of monthly-average daily global, diffuse and beam radiations with hours of bright sunshine in Gebze, Turkey ", *Energy Conversation and Management,* 1996, Vol. 37(9), pp. 1417-1421.

[11]   C. ERTEKIN, O. YALDIZ, "Comparison of some existing models for estimating global solar radiation for Antalya (Turkey)", *Energy Conversation and Management,* 2000, Vol. 41, pp. 311-330.

[12]   AH. HASSAN, "The variability of the daily solar radiation components over Helwan" *Renewable Energy,* 2001, Vol. 23, pp. 641-649.

[13]   A.I. KUDISH, A. LANETZ, "Analysis of the solar radiation data for Beer Sheva, Israil, and its environs", *Solar Energy,* 1992, Vol. 48, pp. 97-106.

[14]   A. SOLER, "The dependence on solar elevation of the correlation between monthly average hourly diffuse and global radiation", *Solar Energy*, 1988,Vol. 41, pp. 335-340.

[15]   H. El AROUDAM, M. El HAMMOUTI, H. EZBAKHE, "Determination of correlations of solar radiation measured in Tetouan", *Renewable Energy,* 1992, Vol. 2, pp. 473-476.

[16]   H.NFAOUI, J.BURET,"Estimation of daily and monthly direct, iffuse and global solar radiation in Rambat(Morocco)", *Renewable Energy,* 1993, Vol. 3(8), pp. 923-930.

[17]   SK. SRIVASTA, OP. SINGH, GN. PANDEY, "Estimation of global solar radiation in Uttar Pradesh (India) and comparison of some existing correlations", *Solar Energy* 1993, Vol.51, pp. 27-29.

[18]   TDMA. SAMUEL, "Estimation of global radiation for Srilanka", *Solar Energy*, 1991, Vol. 47(5), pp. 333.

[19]   K. ULGEN, A. HEPBASLI, "Comparison of solar radiation correlations for Izmir, Turkey", *International Journal of Energy Research,* 2002, Ref No: ER 794, to be published.

[20]   M. GUNES, "Analysis of daily total horizontal solar radiation measurements in Turkey", *Energy Sources,* 2001, Vol. 23,pp. 563-570.

[21]   Z. SEN, A. SAHIN, "Regional assessment of wind power in western Turkey by the cumulative semivariogram method", *Renewable Energy,* 1997, Vol. 12(2), pp. 169-177.

[22]   P. Van LIESHOUT, "Quantifiying risks in wind farm developments", *Proceedings of Wind Energy Symposium*, Pub.13, pp. 115-123, Chamber of Mechanical Engineers Izmir Branch, 2001,Turkey.

[23]   American Wind Energy Atlas

http:// www.awea.org

[24]   Europe Wind Energy Atlas

http://www.ewea.org

[25]   IEA World Energy Outlook, General Projection, 2000.

[26]   BTM Consult ApS,March 2002.

[27]   World Market Update, BTM-C, Chapter2&4, 002.

[28]   O. OZGENER, A. HEPBASLI, "Current status and future directions of wind energy applications in Turkey", *Energy Sources,* 2002, (to be published).

[29]   AB MAYHOUB, A. AZZAM, "A survey on the assessment of wind energy potential in Egypt", *Renewable Energy,* 1997, Vol. 11(2), pp. 235-247.

[30]   D. FERETIC, Z. TOMSIC, N. CAVLINA, "Feasibility analysis of wind energy utilization in Croatia", *Energy* 1999, Vol. 24, pp. 239-246.

[31]   K.MYHJ Othman SOPIAN,   A. WIRSAT, "The wind energy potential of Malaysia. *Renewable Energy* , 1995, Vol. 6(8), pp. 1005-1016.

[32]   R. SHABBANEH, A. Hasan, "Wind energy potential in Palestine. *Renewable Energy,* 1997, Vol. 11(4), pp. 479-483.

[33]   S. REHMAN, TO. HALAWANI, T. HUSAIN, "Weibull parameters for wind speed distribution in Saudi Arabia. *Solar Energy*, 1994, Vol. 53(6), pp. 473-479.

[34]   S. PERSAUD, D. FlLYNN, B. FOX, "Potential for wind generation on the Guyana coastlands", *Renewable Energy,* 199, Vol.18, pp. 175-189.

[35]   A. SAHIN, Z. SEN, "Refined wind energy formulation and its application in Turkey", *The Second International Conference New Energy Systems and Conversions,* 31 July-3 August 1995, pp. 357-360.

[36]   K ULGEN, A. HEPBASLI, "Determination of Weibull parameters for wind energy analysis of Izmir, Turkey", *International Journal of Energy Research,* 2002, Ref No: ER 798, to be published.

[37]   S. INCECIK, F. ERDOGMUS, "An investigation of wind power potential in western coast of Anatolia", *Renewable Energy,* 1994, Vol.6, pp.863-865.

[38]   Y. BORHAN, "Mesoscale. Interactions on wind energy potential in the northern Aegean region: a case study", *Renewable and Sustainable Energy Reviews,* 1998,Vol. 2, pp. 353-360.

[39]   Z. SEN, "Areal assessment of wind speed and topograghy with applications in Turkey", *Renewable Energy,* 2001, Vol.24, pp. 113-129.

[40]   A. SAHIN,"Applicability of wind-solar thermal hybrid power systems in the Northeastern part of the Arabian Peninsula", *Energy Sources,*2000, Vol.22, pp.845-850.

[41] T. MARKVART, *"Solar Electricity"*, 2 th. Edition, John Wiley &Sons, Ltd., New York, 2000.

[42] A. HADI ARAB, B. AIT DRISS, R. AMIMEUR, E. LORENZO, "Photovoltaic systems sizing for Algeria", *Solar Energy,* 1995, Vol. 54(2), pp. 99-104.

[43] J.S. HSIEH., *"Solar Energy Engineering"*, New Jersey Institute of Technology, Prentice-Hall, 1986.

[44] Data Irradiation, 1998.

http://www.anu.edu.au/engn/solar/Sun/Irrad/Irradiation.html.

[45] J. F. KREIDER., C. J. Hoogendoorn, F. Kreith, *"Solar Design Component, System, Economics"*, Hemisphere Publishing Corporation, 1989.

[46] J.F. KREIDER, F. KREITH, *"Solar Energy Handbook"*, McGraw-Hill Book Company, 1991.

[47] J.A. DUFFIE, and W.A. BECKMAN, *"Solar Engineering of Thermal Processes"*, a Willey-Interscience Publication, 1991.

[48] R. MESSENGER, J.VENTRE, *"Photovoltaic Systems Engineering"*, CRC Press, New York, 2000.

[49] G. ATAGUNDUZ, *"Güneþ Enerjisi Temelleri ve Uygulamalarý"*, University of Ege Press, 1989.

[50] Sunlight Design, *"Geography"*, 2002,

http://www.sunlitdesign.com/infosearch/geography.htm#longlat.gif

[51] Sun Angle, 2002 ,

http://www.susdesign.com/sunangle/index.html.

[52] B. OZERDEM, M.H. TURKELI, "Wind energy potential estimation and micrositting on Izmir Institute of Technology Campus, Turkey " , *Int. Journal Energy*, 2003.

[53] B. OZERDEM, M.H. TURKELI, "An Investigation of Wind Characteristics on the Campus of Izmir Institute of Technology ,Turkey", *Int. Journal Renewable*, 2003.

[54] M. M. El- WAKIL, "*Power Plant Technology*", McGraw – Hill Book Company, New York, 1998.

[55] Danish Wind Industry Association, *" Windpower Guided Tour"*, *http://www.Windpower.dk.*

[56]   A. OZDAMAR, N. OZBALTA, E.D. YILDIRIM, "Each of the Wind and Solar Energy Correspandences : Izmir case study ", *National Clean Energy Symphosium,* 15-17 November 2000, Istanbul,Vol. 1.

[57]   M. ENGIN, "Sizing of Wind/Solar Hybrid Energy Production System for Söke", *6 th. Turkish-German Energy Symposium*, 21-24 June 2001, Izmir.

[58]   R. AKKAYA, A.A. KULAKSIZ, "Solar and wind EnergyApplications of Power Electronics" *3 th. International Energy Symposium*, 15-17 November 2000, Istanbul.

[59]   Bergey Wind Power, *"Wind Power Class"*, http://www.bergey.com.

[60]   A. HILAL, Al ISMAILY, P. DOUGLAS, "Photovoltaic Electricity Prospects in oman", *Applied Energy,* 1998,Vol. 59, N. 2-3, pp. 97-124.

[61]   T. MARKVART, " Sizing of Hybrid Photovoltaic Wind Energy System ", *Solar Energy*, October 1996, Vol. 57, Issue 4, pp. 227-281.

[62]   H.M. TURKELI, "An Experimental Investigation of the Parameters to Classify Wind Sites", IZTECH,2002.

[63]   AWS Scientific Inc, "*Wind Resource Assessment Handbook*", New York, 1997.

[64]   J.L. DEBRA, C.B. DENNIS, T.F. LAWRANCE, "Hybrid wind/photovoltaic systems for households in inner Mongolia", *International Conferancew on Village Electrification through Renewable Energy*, 3-5 March 1997, New Delhi.

[65]   Kipp and Zonen *"Instruction Manual CM11 Pyranometer"*

[66]   LI-COR *"LI-1000 Data Logger Instruction Manual"*

[67]   M. GUNES , "Calculation of Solar Radiation on Inclined Surfaces in Turkey", Deprtment of Mechanical Engineering, University of Balýkesir,Turkey,1997.

[68]   T.D.REINDL, "Estimating Diffuse Radiation on Horizontal Surfaces and Total Radiation on Tilted Surfaces", Master of Science Thesis, University of Wisconsin, Madison, 1988.

[69]   Ammonit, "*Choice of Sensors"*, 13-14, Ammonit Wind Measurement Issue, May 2000

http://www.ammonit.de

[70]   Ammonit, *"Wind Measurement for Accurate Energy Predictions"*, *http://www.ammonit.de.*

[71]   Ammonit, *"Data Recording"*, 24-26, Ammonit Wind Measurement Issue, May 2000, *http://www.ammonit.de.*

[72]   Ammonit, *"Data Logger"* , 27-28, Ammonit Wind Measurement Issue, May 2000, *http://www.ammonit.de.*

[73]   Richard BRONSON, Govindasami NADIMUTHU, *"Schaum's outline of Theory and Problems of Operations Research"*, 2th Edition, McGRAW-HILL Company, Newyork, 1997.

[74]   Nesa WU, Richard COPPINS, *"Linear Programming and Extensions"*, McGRAW-HILL Book Company, Newyork, 1981.

[75]   Frederick S. HILLER, Gerald J.LIEBERMAN, *"Introduction to Operations Research"*, 7 th. Edition, McGraw – Hill Book Company, New York, 2001.

[76]   Wayne L. WINSTON, *"Operations Research Applications and Algorithms"* 2 th Printing, PWS-Kent Publishing Company, Boston, 1991.

[77]   K. ULGEN, "A Study on Evaluating Power Generation of Solar –Wind Hybrid Systems in Izmir ,Turkey", *Energy Sources,* Ref No. ES/02/22,2002, Taylor and Francis, USA , 2002.

[78]   M. MUSELLI, G. NOTTON, A. LOUCHE , "Design of hybrid-photovoltaic power generator,with optimiztion of energy managment", *Solar Energy,* 1999, Vol.65, No. 3 pp. 143-157.

[79]   M.A. El-HADIDY, S.M. SHAADID, "Parametric study of hybrid (wind+solar+diesel) power generating systems", *International Journal of Renewable Energy,* 2000, Vol. 21, pp. 129- 139.

[80]   M.A. HABIB, S.A.M. SAID, M.A. El-HADIDY, Al ZAHARNA, "Optimization Procedure of a Hybrid photovoltaic Wind Energy System", *Energy,* 1999, Vol.24, pp. 919-929.

[81]   Mukund R. PATEL, *"Wind and Solar Power Systems"*, CRC Press, New York,1999.

[82]   M.A. El-HADIDY, S.M. SHAADID, "Feasibility of hybrid (wind+solar) power systems for Dhahran, Saudi Arabia", *5 th. World Renewable Energy Congress*, Florence, Italy,1998.

[83]   U.S. Department of Energy Photovoltaics Program "About Photovoltaics", 2002 *http://www.eren.doe.gov/pv/whyuse.html*.

APPENDICIES

APPENDIX A

Table A.1 Hourly,Daily and Monthly Average of Daily Total Radiation at June (*Average Radiation is Max at June During the Year*)

Hour / Day	5-6	6-7	7-8	8-9	9-10	10-11	11-12	12-13	13-14	14-15	15-16	16-17	17-18	18-19	19-20	20-21	Daily Tot.W/m2
1	0.0	0.0	153.0	316.3	483.9	626.6	732.9	824.0	852.5	816.7	732.4	619.6	462.1	288.5	113.4	0.0	**7022.0**
2	0.0	0.0	147.4	316.2	486.1	630.4	747.7	834.9	870.3	843.4	518.2	463.1	473.0	300.2	119.8	0.0	**6750.8**
3	0.0	0.0	147.8	304.7	470.5	623.9	745.3	719.6	701.3	732.7	475.6	396.2	321.6	194.2	74.3	0.0	**5907.3**
4	0.0	0.0	48.6	299.9	489.7	628.4	756.8	637.1	805.8	781.8	376.7	618.5	478.2	308.6	125.7	0.0	**6355.7**
5	0.0	31.9	155.9	320.1	492.3	636.2	737.4	753.3	863.9	840.9	748.0	573.4	338.2	149.1	87.2	0.0	**6727.7**
6	0.0	0.0	144.9	307.5	477.2	616.9	729.2	813.4	843.3	813.7	733.9	621.2	470.6	283.5	94.4	0.0	**6949.5**
7	0.0	0.0	88.9	264.0	457.4	481.2	647.3	538.7	472.6	475.4	359.8	198.8	216.0	103.3	63.7	0.0	**4367.1**
8	0.0	0.0	114.3	310.7	477.6	523.8	558.0	821.0	855.1	843.6	597.7	250.1	178.5	219.7	95.7	0.0	**5845.7**
9	0.0	0.0	136.2	277.6	405.3	624.0	654.5	590.1	714.8	834.9	757.5	642.2	487.2	304.7	128.5	0.0	**6557.4**
10	0.0	0.0	146.5	331.5	508.7	643.2	735.9	811.6	671.8	229.2	515.4	587.7	460.5	300.3	130.2	0.0	**6072.4**
11	0.0	0.0	162.6	334.4	486.9	647.1	746.5	817.8	858.0	832.0	756.1	647.8	501.4	324.8	142.0	0.0	**7257.3**
12	0.0	0.0	155.4	327.7	498.2	637.9	746.5	817.8	854.4	825.7	745.0	629.6	483.0	297.4	128.5	0.0	**7147.0**
13	0.0	0.0	155.9	311.1	482.0	622.8	726.0	798.1	826.4	810.7	733.0	615.0	469.8	301.2	131.1	0.0	**6982.9**
14	0.0	30.8	154.6	322.1	494.3	636.4	742.3	820.8	859.2	836.2	754.0	636.2	487.3	315.5	139.4	0.0	**7228.9**
15	0.0	31.4	157.1	323.2	472.7	603.1	739.1	820.1	861.6	840.6	769.4	618.4	427.8	244.5	146.3	0.0	**7055.3**
16	0.0	33.6	162.4	331.6	507.1	649.5	752.2	828.8	858.0	834.0	755.0	639.1	496.2	326.6	147.0	0.0	**7320.9**
17	0.0	36.4	170.1	339.3	512.2	653.1	763.2	834.8	870.6	845.4	760.2	642.8	495.6	320.8	139.3	0.0	**7383.6**
18	0.0	0.0	150.5	312.9	480.3	617.4	723.4	796.3	831.2	807.9	732.5	630.4	487.5	315.1	139.7	0.0	**7025.1**
19	0.0	35.8	165.5	337.9	503.4	636.9	741.0	815.7	833.0	830.2	759.3	646.5	503.3	335.6	152.9	0.0	**7297.0**
20	0.0	35.9	160.8	324.5	498.5	632.3	738.4	807.3	850.6	823.8	750.9	637.2	496.6	318.8	143.2	0.0	**7218.8**
21	0.0	0.0	162.2	329.8	498.7	639.3	744.0	823.3	856.4	825.2	767.7	614.2	474.8	301.3	135.1	0.0	**7171.8**
22	0.0	29.1	144.1	306.0	475.8	617.6	719.3	796.7	834.8	807.6	729.3	616.8	468.7	307.6	153.7	0.0	**7006.9**
23	0.0	0.0	148.4	313.2	482.4	622.9	724.6	796.1	830.0	802.6	729.6	628.9	490.8	320.4	146.8	0.0	**7036.5**
24	0.0	0.0	142.7	312.3	481.6	624.7	737.2	815.3	858.6	837.5	764.9	648.0	496.5	315.9	138.1	0.0	**7173.3**
25	0.0	0.0	133.1	297.8	463.1	606.1	711.3	784.3	804.2	534.0	570.6	627.0	480.2	321.0	150.2	0.0	**6482.8**
26	0.0	0.0	144.9	307.8	481.8	624.9	727.9	816.5	855.4	833.4	751.5	637.2	488.6	311.8	136.1	0.0	**7117.8**
27	0.0	0.0	136.4	297.3	460.6	600.9	706.7	785.1	820.0	798.5	728.3	623.0	485.9	315.9	137.4	0.0	**6895.8**
28	0.0	0.0	137.3	307.9	479.9	618.0	723.1	798.2	833.8	813.9	739.5	637.9	497.3	324.5	144.3	0.0	**7055.4**
29	0.0	0.0	147.9	322.2	495.2	636.0	742.2	827.4	857.9	825.7	741.7	638.8	486.3	302.2	128.1	0.0	**7151.6**
30	0.0	0.0	124.4	295.0	467.5	616.0	726.8	804.2	829.0	796.5	726.6	620.9	482.2	311.9	138.3	0.0	**6939.2**
Avg.	**0.0**	**8.8**	**143.3**	**313.4**	**482.4**	**619.2**	**724.2**	**784.9**	**817.8**	**779.1**	**686.0**	**586.9**	**452.9**	**289.5**	**128.3**	**0.0**	**6816.8 Wh/m²-day**

Table A.2 Hourly, Daily and Monthly Average of Daily Total Radiation at December (*Average Radiation is Min at December During the Year*)

Hour / Day	5-6	6-7	7-8	8-9	9-10	10-11	11-12	12-13	13-14	14-15	15-16	16-17	17-18	18-19	19-20	20-21	Daily Total W/m2
1	0.0	0.0	0.0	77.2	201.0	298.9	368.7	380.5	331.0	178.3	75.5	13.2	0.0	0.0	0.0	0.0	**1924.3**
2	0.0	0.0	0.0	8.7	42.6	55.3	50.2	30.8	23.0	30.2	19.8	0.0	0.0	0.0	0.0	0.0	**260.7**
3	0.0	0.0	0.0	73.4	94.1	153.5	367.1	233.4	169.8	45.0	45.3	20.5	0.0	0.0	0.0	0.0	**1201.9**
4	0.0	0.0	0.0	57.8	73.3	88.5	92.6	87.5	178.1	160.7	68.6	8.6	0.0	0.0	0.0	0.0	**815.8**
5	0.0	0.0	0.0	16.7	31.9	17.5	167.4	257.1	145.4	112.3	44.1	4.9	0.0	0.0	0.0	0.0	**797.4**
6	0.0	0.0	0.0	79.8	111.3	145.6	94.3	269.6	123.2	38.9	40.6	24.7	0.0	0.0	0.0	0.0	**928.0**
7	0.0	0.0	0.0	0.0	36.2	58.7	73.9	63.4	56.0	6.1	12.7	0.0	0.0	0.0	0.0	0.0	**307.1**
8	0.0	0.0	0.0	13.0	23.5	35.8	33.7	19.4	13.9	12.3	6.7	0.0	0.0	0.0	0.0	0.0	**158.3**
9	0.0	0.0	0.0	12.0	71.5	142.3	178.1	150.9	137.4	130.1	102.8	54.0	0.0	0.0	0.0	0.0	**979.0**
10	0.0	0.0	0.0	52.5	223.5	323.5	381.8	386.2	352.6	285.8	185.5	38.8	0.0	0.0	0.0	0.0	**2230.0**
11	0.0	0.0	0.0	95.3	219.4	321.9	382.4	395.6	351.2	268.5	162.8	41.2	0.0	0.0	0.0	0.0	**2238.2**
12	0.0	0.0	0.0	101.0	190.1	317.2	371.1	382.5	292.9	213.9	123.3	35.6	0.0	0.0	0.0	0.0	**2027.6**
13	0.0	0.0	0.0	47.7	159.9	126.5	87.0	89.1	93.3	68.1	50.8	14.9	0.0	0.0	0.0	0.0	**737.1**
14	0.0	0.0	0.0	6.1	18.2	29.3	50.2	51.4	82.7	90.1	25.7	11.4	0.0	0.0	0.0	0.0	**365.2**
15	0.0	0.0	0.0	87.2	202.4	304.7	366.6	382.9	350.0	270.3	158.1	38.6	0.0	0.0	0.0	0.0	**2160.8**
16	0.0	0.0	0.0	72.2	185.2	233.9	348.8	392.4	348.8	277.3	167.3	40.0	0.0	0.0	0.0	0.0	**2065.9**
17	0.0	0.0	0.0	18.5	93.8	216.3	359.6	380.6	345.8	276.3	161.5	41.5	0.0	0.0	0.0	0.0	**1893.7**
18	0.0	0.0	0.0	70.7	159.1	187.6	244.4	180.9	175.5	94.6	77.4	17.6	0.0	0.0	0.0	0.0	**1207.8**
19	0.0	0.0	0.0	15.2	24.8	34.7	127.5	204.4	195.4	274.4	125.3	53.7	0.0	0.0	0.0	0.0	**1055.4**
20	0.0	0.0	0.0	93.1	202.8	319.1	208.5	158.5	66.6	136.2	105.9	26.8	0.0	0.0	0.0	0.0	**1317.4**
21	0.0	0.0	0.0	75.7	195.5	302.1	369.2	384.7	353.3	278.2	164.6	46.4	0.0	0.0	0.0	0.0	**2169.5**
22	0.0	0.0	0.0	105.7	238.3	301.3	370.2	389.3	361.0	284.3	172.8	47.0	0.0	0.0	0.0	0.0	**2269.8**
23	0.0	0.0	0.0	109.6	198.7	287.3	342.1	337.9	336.1	210.0	116.5	26.2	0.0	0.0	0.0	0.0	**1964.4**
24	0.0	0.0	0.0	28.5	121.8	118.4	214.6	391.8	355.2	282.1	179.7	23.8	0.0	0.0	0.0	0.0	**1715.9**
25	0.0	0.0	0.0	54.9	117.5	239.6	332.6	337.5	352.1	293.3	134.1	37.3	0.0	0.0	0.0	0.0	**1898.9**
26	0.0	0.0	0.0	60.5	200.4	294.0	342.8	402.0	355.6	185.8	57.1	25.1	0.0	0.0	0.0	0.0	**1923.4**
27	0.0	0.0	0.0	23.7	91.0	141.1	118.3	117.6	63.0	64.2	49.3	15.0	0.0	0.0	0.0	0.0	**683.3**
28	0.0	0.0	0.0	20.6	95.4	211.3	327.8	83.5	222.7	178.0	147.0	38.0	0.0	0.0	0.0	0.0	**1324.3**
29	0.0	0.0	0.0	32.6	111.8	101.6	128.1	94.6	75.7	71.1	88.7	27.1	0.0	0.0	0.0	0.0	**731.4**
30	0.0	0.0	0.0	20.8	72.2	309.7	244.1	352.0	259.6	308.5	145.2	57.1	0.0	0.0	0.0	0.0	**1769.1**
31	0.0	0.0	0.0	88.3	113.8	181.6	332.6	298.6	117.0	244.0	133.9	21.9	0.0	0.0	0.0	0.0	**1531.8**
Avg.	**0.0**	**0.0**	**0.0**	**52.2**	**126.5**	**190.3**	**241.2**	**248.0**	**215.6**	**173.2**	**101.6**	**27.5**	**0.0**	**0.0**	**0.0**	**0.0**	**1375.9 Wh/m2-day**

Table A.3 Daily Radiation for the Months from January to December.

Day	January	February	March	April	May	June	July	August	September	October	November	December
1	285	2813	3706	883	6198	7066	6824	6308	3569	3387	2820	1924
2	1557	2554	3748	4073	6479	6796	6710	6269	3093	3995	2955	261
3	1306	2942	4196	4216	6649	5957	6906	6485	4049	3969	2668	1202
4	183	2859	3435	950	6815	6374	6542	6513	5331	4020	2112	816
5	1988	1544	3269	2115	6706	6749	6851	6393	4906	3893	1172	797
6	907	2382	3773	3817	6498	6999	6700	6459	5183	3891	1520	928
7	2340	2502	3801	4970	6533	4426	7000	6459	5161	2817	1979	307
8	2075	2665	3107	5682	4307	5893	6936	6479	4495	3510	1627	158
9	1813	2078	3637	5276	5298	6611	6572	6358	3924	3484	1553	979
10	2396	1426	2620	5259	6619	6127	6861	6476	3223	3938	2092	2230
11	2363	1392	858	4979	6542	7300	6466	5899	5044	2804	2269	2238
12	2437	3439	1728	3119	6429	7200	6709	4728	3017	2126	2827	2028
13	2030	3394	3054	2858	3195	7039	6655	6262	2974	1804	2842	737
14	774	3320	1881	5575	5660	7244	7001	6050	2899	2214	2674	365
15	2074	1592	4349	3381	7019	7070	7037	6288	1982	3130	0	2161
16	1709	3330	4518	1806	7071	7333	6574	4997	3537	3771	0	2066
17	1276	3525	4153	2886	6807	7399	6929	5467	4577	3795	0	1894
18	692	3293	4497	4135	6905	7073	7034	5808	5127	3778	0	1208
19	608	2872	4794	2624	7281	7312	7121	5884	5044	3357	0	1055
20	615	2145	1964	4029	7281	7234	6656	5929	5009	3304	2645	1317
21	1897	2824	4723	5178	6615	7228	6805	5789	4917	3714	1526	2170
22	2299	3527	3971	5843	6800	7023	6893	5999	4853	3658	1341	2270
23	2653	796	1308	6122	6842	7087	6587	6080	4429	2454	2379	1964
24	1734	3270	1503	5975	7148	7227	6977	5839	2961	3060	2532	1716
25	883	3675	1140	6287	4971	6528	6153	5776	2380	3432	2283	1899
26	1783	3861	4362	6333	2793	7171	6687	5775	4098	3493	2034	1923
27	2392	3279	3755	6306	6638	6946	6151	5659	4647	2920	2250	683
28	2771	1519	4945	4690	6832	7099	4470	5603	3409	3398	1834	1324
29	2869		3879	4004	6146	7204	6662	5221	1081	3513	2197	731
30	2931		4941	4271	5248	6986	6017	5186	2570	3421	1829	1769
31	2981		5138		6689		7046	2574		3330		1532
Avg. Wh/m²-day	**1762,0**	**2671,9**	**3443,6**	**4254,8**	**6226,3**	**6856,7**	**6662,4**	**5839,1**	**3916,2**	**3334,9**	**1798,8**	**1375,9**

Table A.4 Monthly Average of Daily Total Diffuse Radiation and Clearness Index

| Month	H (kWh/ m2-day)	Hd (kWh/m2-day)	Ho (kWh/m2-day)	Clearnes Index KT	Hd / H
January	1.74	0.85	4.58	0.38	0.49
February	2.65	1.11	5.94	0.45	0.42
March	3.42	1.47	7.86	0.44	0.43
April	4.23	1.82	9.75	0.43	0.43
May	6.19	2.00	11.06	0.56	0.32
June	6.82	2.06	11.58	0.59	0.30
July	6.66	2.01	11.31	0.59	0.30
August	5.84	1.85	10.25	0.57	0.32
September	3.92	1.59	8.53	0.46	0.41
October	3.33	1.21	6.53	0.51	0.36
November	1.80	0.90	4.89	0.37	0.50
December	1.38	0.76	4.17	0.33	0.55
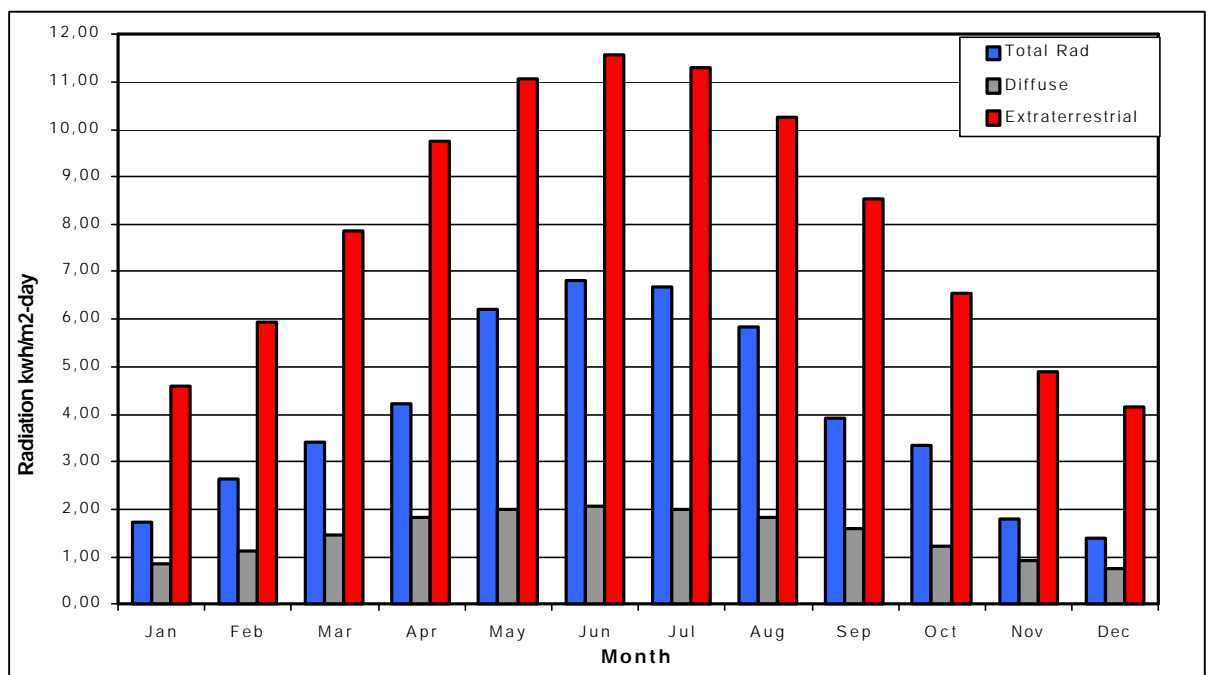
Figure A.1 Monthly Average of Daily Total, Diffuse and Extraterrestrial Radiation on Horizontal Surface.

APPENDIX B

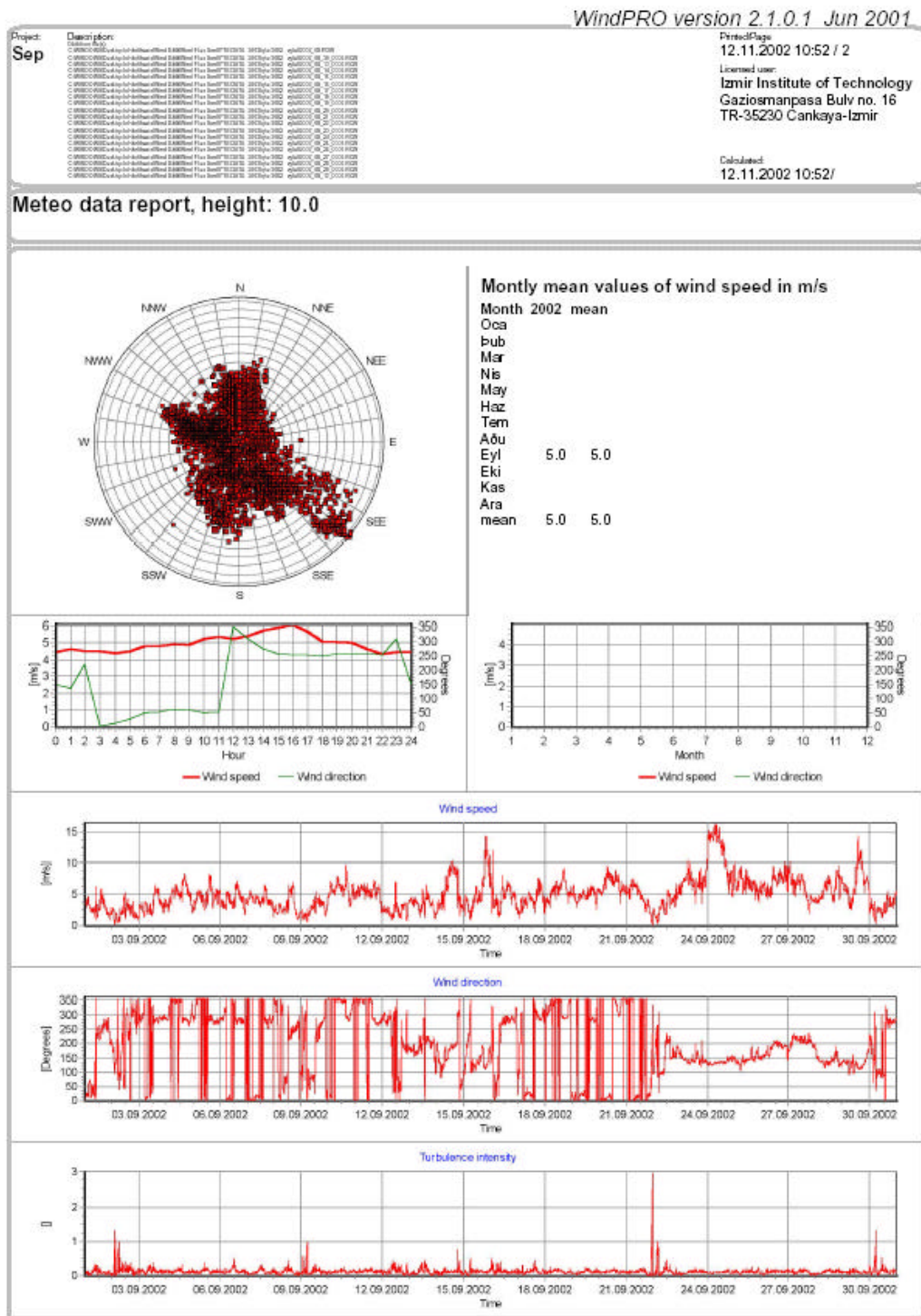**Figure B.1** Turbulance Intensity of Wind Speed for September

Figure B.2 Weibull Distribution of Wind speed for September

Meteo data report, height: 10.0

Weibull Data

k-parameter correction: 0.0080/m

Sector	A- parameter [m/s]	Mean wind speed [m/s]	k- parameter	Frequency	Frequency [%]	Wind shear
0-N	5.50	4.98	3.928	19.54	19.5	0.17
1-NNE	4.59	4.08	2.620	5.51	5.5	0.15
2-ENE	2.98	2.68	3.315	1.94	1.9	0.06
3-E	3.05	2.71	2.534	4.49	4.5	0.03
4-ESE	8.97	7.94	2.073	8.84	8.8	0.11
5-SSE	7.01	6.24	2.785	12.90	12.9	0.19
6-S	6.21	5.50	2.440	8.03	8.0	0.03
7-SSW	5.64	5.00	2.282	7.94	7.9	0.07
8-WSW	3.91	3.47	1.878	3.15	3.1	0.06
9-W	4.70	4.21	3.178	10.05	10.0	0.10
10-WNW	5.04	4.47	2.320	12.23	12.2	0.11
11-NNW	4.73	4.20	2.665	5.37	5.4	0.13
mean	5.67	5.02	2.106	100.00	100.0	0.12

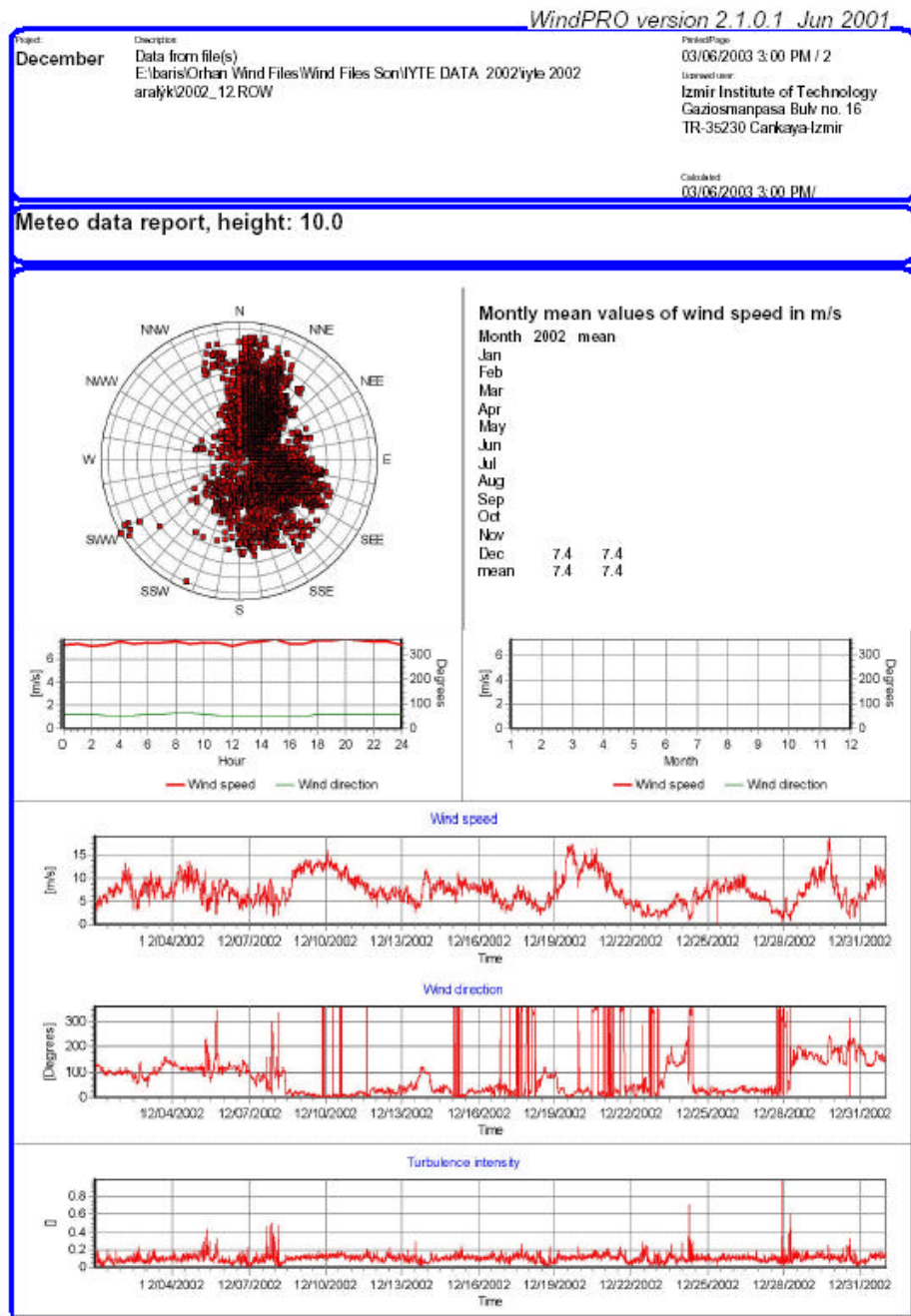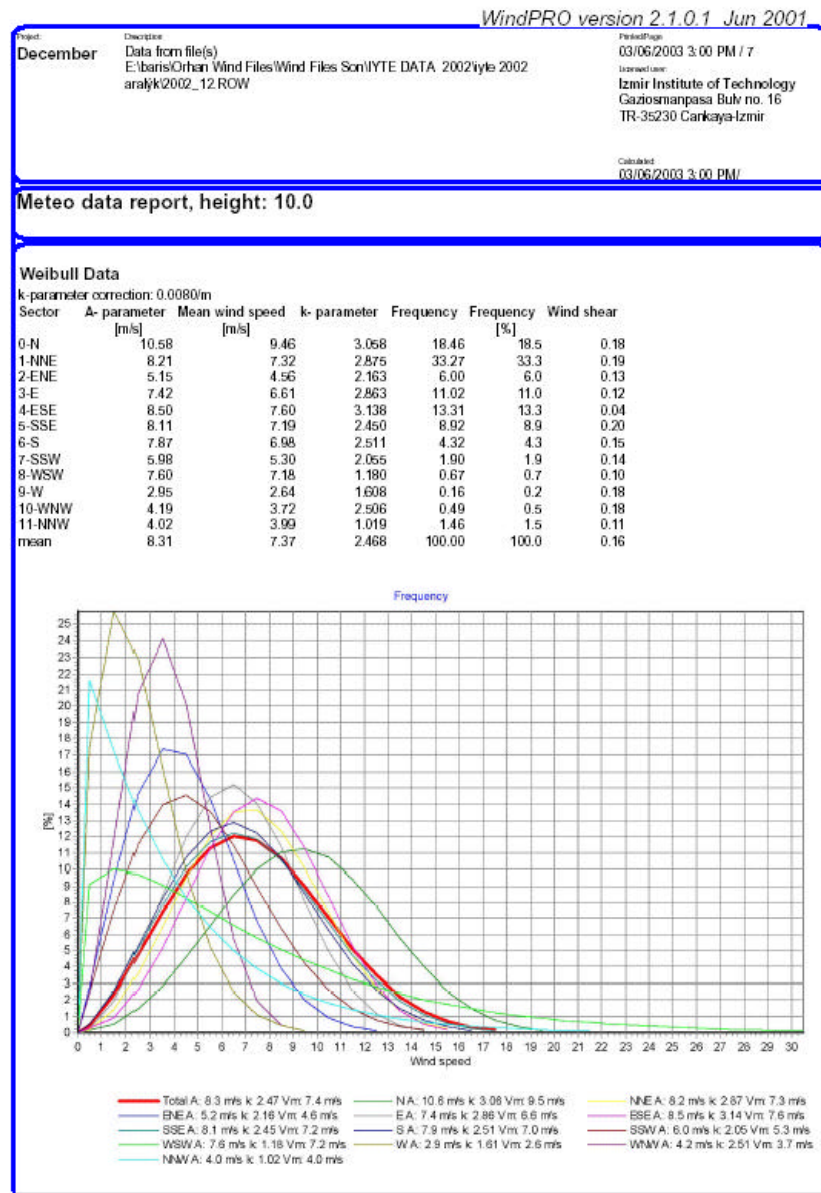**Figure B.3** Turbulance Intensity of Wind Speed for December

Figure B.4 Weibull Distribution of Wind speed for December

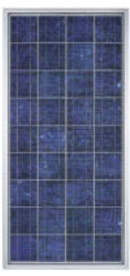# APPENDIX C

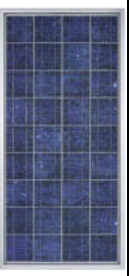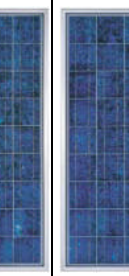**Table C.1** Shell Solar and Siemens PV Cells Specifications
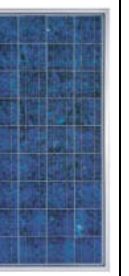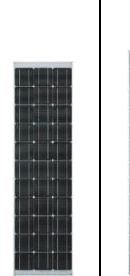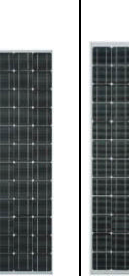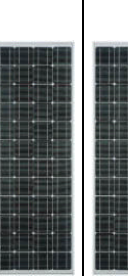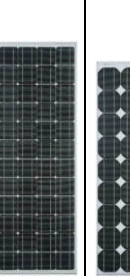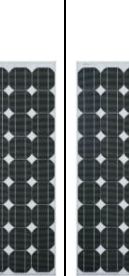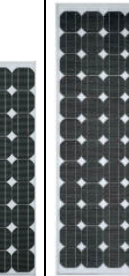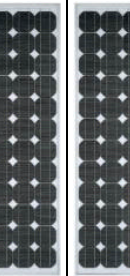
Specifications	S 70	S 75	S 105	S 115	SM 50-H	SM 55	SM 110-12	SM110-24	SP 70	SP 75	SP 140	SP 150
Number of Cells	36	36	54	54	36	36	72	72	36	36	72	72
Type of Cells	Poly Crystal	Poly Crystal	Poly Crystal	Poly Crystal	Mono Crystal	Mono Crystal	Mono Crystal	Mono Crystal	Mono Crystal	Mono Crystal	Mono Crystal	Mono Crystal
Dimensions of Cells	125 x 125	125 x 125	125 x 125	125 x 125	103 x 103	103 x 103	103 x 103	103 x 103	125 x 125	125 x 125	125 x 125	125 x 125
Max Power	70 W	75 W	105 W	115 W	50 W	55 W	110 W	110 W	70 W	75 W	140 W	150 W
Nominal Power (U)	12 V	12 V	18 V	18 V	12 V	12 V	12 V	24 V	12 V	12 V	24 V	24 V
Max Voltage (Up)	21.2 V	21.6 V	31.8 V	32.8 V	19.8 V	21.7 V	21.7 V	43.5 V	21.4 V	21.7 V	42.8 V	43.4 V
Current (Isc)	4.50 A	4.70 A	4.50 A	4.70 A	3.35 A	3.45 A	6.90 A	3.45 A	4.70 A	4.80 A	4.70 A	4.80 A
Height (H)	1220 mm	1220 mm	1220 mm	1220 mm	1219 mm	1293 mm	1316 mm	1316 mm	1200 mm	1200 mm	1619.4 mm	1619.4 mm
Lenght (L)	580 mm	580 mm	850 mm	850 mm	329 mm	329 mm	660 mm	660 mm	527 mm	527 mm	814 mm	814 mm
Width (W)	54 mm	54 mm	54 mm	54 mm	34 mm	34 mm	54 mm	54 mm	56 mm	56 mm	54 mm	54 mm
Thickness (t)	25 mm	25 mm	25 mm	25 mm	34 mm	34 mm	40 mm	40 mm	34 mm	34 mm	40 mm	40 mm
Weight (W)	10 kg	10 kg	14 kg	14 kg	5.2 kg	5.5 kg	11.5 kg	11.5 kg	7.6 kg	7.6 kg	14.8 kg	14.8 kg
Peak Power Warranty	20 years	20 years	20 years	20 years	25 years	25 years	25 years	25 years	25 years	25 years	25 years	25 years

Table C.2 Bergey,Ampair,Southwest Wind Turbine Specifications.

Producer	Model	Power (W)	Blade Diameter (m)	Voltage (Volt)	Speed (m/ s)	Weight (Kg)
Fortis	Yellow Sand	200	2,0	24	3 - 8	45
Fortis	Yellow Sand	300	2,4	24	3 - 8	55
Fortis	Yellow Sand	500	2,5	24	3 - 9	65
Fortis	Espada	800	2,2	12-24	3 - 16	55
Fortis	Passaat	1.400	3,1	12-24	3 - 15	75
Fortis	Montana	5.000	5,00	24-48	3 - 17	200
Fortis	Alize	10.000	7,00	120	3 - 13	600
Fortis	Boreas	30.000	14,00	400	3 - 12	1950
Bergey	XL.1	1.000	2,5	24	3 - 11	45
Bergey	BWC 1500	1.500	3,0	12-24-48	3 - 13	80
Bergey	Excel-R7.5	7.500	7,0	24-48-120	3 - 15	550
Bergey	Excel-S10	10.000	7,0	230	3 - 15	550
Bergey	XL.50	50.000	14,0	400	3 - 11	1900
Ampair	Hawk	100	0,95	12-24	3 - 12	13
Ampair	Pacific	100	0,95	12-24	3 - 12	13
Ampair	Aquair	100	*wave*	12-24	*wave*	--
Ampair	Aquair	100	*wave*	12-24	*wave*	--
Southwest	Air 403L	400	1,15	12-24-48	3 - 12	6
Southwest	Air 403M	400	1,15	12-24-48	3 - 12	6

Table C.3 Charge Regulator Specifications

Producer	Model	Specifications
Steca	Solsum 5.0	5 Amper Charge Controlar (12&24 V)
Steca	Solsum 6.6X	6 Amper Charge Controlar (12&24 V)
Steca	Solsum 8.8X	8 Amper Charge Controlar (12&24 V)
Steca	Solarix Zeta	8 Amper Charge Controlar (12&24 V)
Steca	Solarix Jota	12 Amper Charge Controlar (12&24 V)
Steca	Solarix Delta	20 Amper Charge Controlar (12&24 V)
Steca	Solarix Theta	30 Amper Charge Controlar (12&24 V)
Steca	Tarom 235	35 Amper Charge Controlar (12&24 V)
Steca	Tarom 245	45 Amper Charge Controlar (12&24 V)
Steca	Tarom 430	30 Amper Charge Controlar (48 V)
Phocos	PL20	20 Amper Charge Controlar (12 - 48 V)
Phocos	PL60	60 Amper Charge Controlar (12 - 48 V)

Table C.4 Inverter Specifications

Producer	Model	Specifications
Steca	Sinusoidal	550W, 12Vdc-230Vac, Chargeble
Steca	Sinusoidal	900W, 24Vdc-230Vac, ª arj Chargeble
ASP	TC1,5/12	150W, 12Vdc-230Vac, Inverter
ASP	TC05/12	500W, 12Vdc-230Vac, Inverter
ASP	TC08/12	800W, 12Vdc-230Vac, Inverter
ASP	TC13/12	1300W, 12Vdc-230Vac, Inverter
ASP	TC20/12	2000W, 12Vdc-230Vac, Inverter
ASP	TC2,5/24	250W, 24Vdc-230Vac, Inverter
ASP	TC07/24	700W, 24Vdc-230Vac, Inverter
ASP	TC10/24	1000W, 24Vdc-230Vac, Inverter
ASP	TC13/24	1300W, 24Vdc-230Vac, Inverter
ASP	TC20/24	2000W, 24Vdc-230Vac, Inverter
ASP	TC30/24	3000W, 24Vdc-230Vac, Inverter
ASP	TC08/48	800W, 48Vdc-230Vac, Inverter
ASP	TC22/48	2200W, 48Vdc-230Vac, Inverter
ASP	TC35/48	3500W, 48Vdc-230Vac, Inverter
Xantrex	150i	150W, 12Vdc-230Vac, Inverter
Xantrex	300i	300W, 12Vdc-230Vac, Inverter
Xantrex	500i	500W, 12Vdc-230Vac, Inverter

APPENDIX D

Mathlab Code of Monthly Average of Daily Total Extraterrestrial Radiation on Horizontal Surface:

```
nn=0;
Htot=0;
Ho=zeros(400,1);
Haverage=zeros(12,1);
c=zeros(12,1);
for i=1 :12
c=input('Number of Month=');
c(i,1)=i;
d=input('Total Day of Month =');
lat=38
for n = 1:d
a = (360 / 365) * (284 + (nn + n));
dec = 23.45 * sin(a * 3.14 / 180);
suns = (acos(-tan(lat * 3.14 / 180) * tan(dec * 3.14 / 180)))* 180 /
3.14;
Gsc = 1367;
Ho(n,1) = (24 * Gsc * 0.0036 / 3.14) * (1 + 0.033 * cos(360 * 3.14 *
(n + nn) / (365 * 180))) * (cos(lat * 3.14 / 180) * cos(dec * 3.14 /
180) * sin(suns * 3.14 / 180) + (3.14 * suns / 180) * sin(lat * 3.14 /
180) * sin (dec * 3.14 / 180));
Htot = Htot + Ho(n,1);
n
nn
dec
suns
'Ho for day'
Ho(n,1)
end
Htot
Haverage(i,1) = Htot / d;
'month'
c(i,1)
'Monthly average of daily total extraterrestrial rad. on horizontal'
Haverage(i,1)
nn=nn + d
Htot=0;
end
plot(c,Haverage)
'Finish'
```

Mathlab Code of Monthly Average of Daily Total Radiation on Tilted Surface:

```
c=zeros(12,1);
Ho=zeros(12,1);
H=zeros(12,1);
HT=zeros(12,1);
for i=1 : 12
c=input('number of month=');
Ho=input('monthly average of daily tot extraterrestrial on horiz.
Ho=');
Ho(i,1)=Ho;
H=input('monthly average of daily tot on horiz.(measured value) H=');
H(i,1)=H;
lat=38;
N=input('average day of (year)the month=');
ro=input('RO=');
a = (360 / 365) * (284 + (N));
dec = 23.45 * sin(a * 3.14 / 180);
beta =lat;
%beta = (lat) - (1.5 * dec) - ( abs(dec) *  lat / 180);
suns = (acos(-tan(lat * 3.14 / 180)* tan(dec * 3.14 /180))) * 180 /
3.14;
b = (acos(-tan((lat - beta) * 3.14 / 180) * tan(dec * 3.14 / 180)))*
180 / 3.14;
if b < suns
sunst = b;
else
sunst = suns;
end

%All of them are monthly average of daily total value
RB = (cos((lat - beta) * 3.14/ 180) * cos(dec * 3.14 / 180) *
sin(sunst * 3.14 / 180) + (3.14 / 180) * sunst * sin((lat - beta) *
3.14 / 180) * sin(dec * 3.14 / 180)) / (cos(lat * 3.14 / 180) *
cos(dec * 3.14 / 180) * sin(sunst * 3.14 / 180) + (3.14 / 180) * suns
* sin(lat * 3.14 / 180) * sin(dec * 3.14 / 180));
KT = H(i,1) / Ho(i,1);
Hd = H(i,1) * (1.39 - 4.027 * KT + 5.531 * (KT ^ 2) - 3.108 * (KT ^
3))
R = (1 - (Hd / H(i,1))) * RB + (Hd / H(i,1)) * (1 + (cos(beta * 3.14 /
180))) / 2 + ro * ((1 - (cos(beta * 3.14 / 180))) / 2);

lat
N
Ho(i,1)
H(i,1)
ro
beta
dec
suns
sunst
RB
KT
R
HT(i,1) = H(i,1) * R;
'Month'c
'Tilted surface Monthly Average of Daily total Radiation'
HT(i,1)
end
'Finish'
```

Lindo Code

Wind / PV Hybrid System Optimization

MIN $3a_W + 5.8a_S$ minimize the hybrid cost

SUBJECT TO

JAN) $2.7a_S + 2.5a_W >= 15.3$
FEB) $3.7a_S + 2.6a_W >= 17.7$
MARC) $4.0a_S + 3.2a_W >= 14.5$
APR) $4.3a_S + 2.8a_W >= 18.5$
MAY) $5.5a_S + 2.1a_W >= 25.2$
JUNE) $5.7a_S + 3.6a_W >= 22.5$
JULY) $5.7a_S + 2.6a_W >= 22.5$
AUG) $5.6a_S + 3.5a_W >= 32.4$
SEP) $4.3a_S + 1.7a_W >= 18.3$
OCT) $4.5a_S + 2..6a_W >= 22.5$
NOV) $2.7a_S + 2.3a_W >= 18$
DEC) $2.1a_S + 4.3a_W >= 20.9$
$a_S > 0$
$a_W > 0$
END